Titre: Title:	Numerical Study of Sediment and Chemical Transport in the Lower Athabasca River Due to a Tailings Dam Breach Spill and in the Context of Climate Change
Auteur: Author:	Maryam Taherparvar Pahmedani
Date:	2022
Type:	Mémoire ou thèse / Dissertation or Thesis
Référence: Citation:	Taherparvar Pahmedani, M. (2022). Numerical Study of Sediment and Chemical Transport in the Lower Athabasca River Due to a Tailings Dam Breach Spill and in the Context of Climate Change [Mémoire de maîtrise, Polytechnique Montréal]. PolyPublie. https://publications.polymtl.ca/10468/

POLYTECHNIQUE MONTRÉAL

affiliée à l'Université de Montréal

Numerical study of sediment and chemical transport in the Lower Athabasca River due to a tailings dam breach spill and in the context of climate change

Maryam TAHERPARVAR PAHMEDANI

Département des génies civil géologique et des mines

Mémoire présenté en vue de l'obtention du diplôme de *Maîtrise ès sciences appliquées*

Génie Civil

Août 2022

POLYTECHNIQUE MONTRÉAL

affiliée à l'Université de Montréal

Ce mémoire intitulé :

Numerical study of sediment and chemical transport in the Lower Athabasca River due to a tailings dam breach spill and in the context of climate change

présenté par **Maryam TAHERPARVAR PAHMEDANI**

en vue de l'obtention du diplôme de *Maîtrise ès sciences appliquées*
a été dûment accepté par le jury d'examen constitué de :

Elmira HASSANZADEH, présidente

Ahmad SHAKIBAEINIA, membre et directeur de recherche

Sarah DORNER, membre

DEDICATION

After a long time, after walking many paths with the sweet presence of my dear teachers,

I am grateful to my honorable professors for all their support and unstinting efforts. I am very grateful to my supervisor, Professor Shakibaeinia, who took the trouble of judging this thesis,

With their guidance and many concerns and the beautiful mischief of that time, the looks of my parents,

With eyes full of excitement, and the beauty of my husband's presence by my side, which has turned the fatigue of this road into hope and light.

And I hope to be able to respond to all their love in the near future...

Now, with great respect for all these dear people's efforts for my success….

I dedicate this thesis to my dear sister, my parents and dear professors

I hope to be able to understand the beauty of their existence

Thanks …

RÉSUMÉ

Les barrages de résidus sont connus pour causer des accidents et ont déjà été la cause d'accidents mortels. Maintenant que cette question est posée, quelles seront les conséquences de la rupture possible des digues à résidus, et ces effets persisteront-ils au fil du temps ? Ces barrages offrent la possibilité de stocker à grande échelle et pour une longue durée les déchets issus du processus d'extraction minière. Rien qu'au cours du siècle actuel, qui s'est écoulé depuis près de 2 décennies, 11 ruptures graves de ces barrages ont été signalées, et il semble que ce nombre soit en augmentation. Dans le même temps, la probabilité de défaillance et d'effondrement des digues à résidus est plus élevée que dans les barrages hydrauliques, et cela s'explique par leur utilisation industrielle.

Les barrages hydrauliques sont des structures fiables qui sont utilisées pour stocker l'eau et être efficaces dans son utilisation, tandis que les barrages à résidus sont utilisés pour stocker les résidus qui ne sont pas nécessaires. En conséquence, nous préférons dépenser le moins d'argent pour leur construction. Pour répondre à la question de savoir pourquoi une digue à résidus s'effondre, plusieurs raisons peuvent être avancées, telles que le poids imposé à la digue à la suite de fortes pluies et la faiblesse des fondations de la digue. De plus, la transformation des déchets solides en une substance liquide peut entraîner le rejet de déchets à la surface de l'eau et dans les eaux souterraines, ce qui constitue une menace pour la faune.

De nombreuses ruptures catastrophiques historiques de barrages de résidus au Canada ont soulevé des inquiétudes quant aux risques associés aux résidus de sables bitumineux, tels que la sécurité et les impacts environnementaux. Par conséquent, il a augmenté l'intérêt d'étudier les effets potentiels de la rupture d'un barrage de résidus de sables bitumineux sur la qualité de l'eau ainsi que sur les terres adjacentes dans la zone en aval.

L'étude et la modélisation de l'écoulement après la rupture des digues à résidus créent leurs propres difficultés en raison du comportement non newtonien des matériaux de résidus. Cette étude vise à étudier numériquement le flux de résidus de rupture de barrage sur les barrages de résidus de sables bitumineux.

Cette étude se compose de deux parties principales. Dans la première partie, les conséquences possibles d'une défaillance hypothétique du barrage de résidus de sables bitumineux sont discutées en effectuant une simulation numérique de l'écoulement souterrain, y compris les conditions d'inondation et les fuites subséquentes vers les eaux voisines. le bassin de décantation du lac Mildred (MLSB) est représentatif de la zone de sables bitumineux du bas Athabasca sélectionnée. À cette fin, le modèle EFDC (Environmental Fluid Dynamics Code) a été utilisé. Un modèle hydrodynamique qui permet de modéliser le comportement hydrodynamique et l'aspect non newtonien des écoulements résultant de la rupture des digues à résidus.

Dans la deuxième partie, sur la base des données sur le changement climatique, cinq hypothèses de rupture de digues à résidus ont été simulées pour l'avenir. Les simulations ont été réalisées sur des périodes de 30 jours, et cette période de 30 jours permet d'étudier le comportement des sédiments durant cette période.

Il a été constaté qu'une partie importante des résidus déversés quittera le domaine de simulation en aval et que le reste sera déposé dans le lit de la rivière. Ces changements sont plus importants en cas de changement climatique. En cas d'inondation ultérieure, le matériau déposé sera remis en suspension, ce qui entraînera une autre augmentation de la concentration de sédiments/produits chimiques dans la colonne d'eau.

ABSTRACT

Tailings dams are notorious for causing accidents and have been the cause of fatal accidents before. Now this question is raised, what consequences will befall us due to the possible failure of tailings dams, and will these effects still remain over time? These dams provide the possibility of storing wastes from the mineral extraction process on a large scale and for a long time. Only in the current century, which has passed nearly 2 decades, 11 serious breaks in these dams have been reported, and it seems that this number is increasing. At the same time, the probability of failure and collapse of tailings dams are higher than in water dams, and the reason for this is their industrial use.

Water dams are reliable structures that are used to store water and be efficient in its use, while tailings dams are used to store residues that are not needed. As a result, we prefer to spend the least amount of money on their construction. To answer the question of why a tailings dam collapses, several reasons can be put forward, such as the weight that is imposed on the dam as a result of heavy rains and the weak foundation of the dam. Also, the transformation of solid waste into a liquid substance can lead to the discharge of waste to the water surface and underground water, which is a threat to wildlife.

Many historic catastrophic tailings dams failures in Canada have raised concerns about the risk associated with oil-sands tailings, such as safety and environmental impacts. Therefore, it has increased the interest to investigate the potential effects of the failure of an oil sand tailings dam on the water quality as well as the adjacent lands in the downstream area.

Studying and modeling the flow after the failure of tailings dams creates its own difficulties due to the non-Newtonian behavior of tailings materials. This study aims to numerically investigate the flow of dam breach tailings on oil sands tailings dams.

This study consists of two main parts. In the first part, the possible consequences of a hypothetical failure of the oil sand tailings dam are discussed by conducting a numerical simulation of the ground flow, including flood conditions and the subsequent leakage to nearby waters. the Mildred Lake Settling Basin (MLSB) tailings pond is a representative of the lower Athabasca oil sands area selected. For this purpose, The Environmental Fluid Dynamics Code (EFDC) model was used. A

hydrodynamic model that can model the hydrodynamic behavior and the non-Newtonian aspect of flows resulting from the failure of tailings dams.

In the second part, based on climate change data, five tailings dam failure hypotheses were simulated for the future. The simulations were performed in 30-day periods, and this 30-day period allows the behavior of sediments to be investigated during this period.

It was found that a significant portion of spilled tailing material will leave the simulation domain downstream, and the rest will be deposited within the riverbed. These changes are more significant under changing climate. Should subsequent flooding happens the deposited material will be resuspended, resulting in another increase in the sediment/ chemical concentration in the water column.

TABLE OF CONTENTS

LIST OF TABLES

LIST OF FIGURES

LIST OF SYMBOLS AND ABBREVIATIONS

LAR	Lower Athabasca River
MLSB	Mildred Lake Settling Basin
TSFs	Tailing Storage Facilities
OSPW	Oil-Sands Process-affected Water
MFT	Mature Fine Tailings
FFT	Fine Fluid Tailings
PAHs	Polycyclic Aromatic Hydrocarbons
SSC	Suspended Sediment Consentration
TSS	Total Suspended Sediment
DS MLSB	DownStream of MLSB
DS Firebag	DownStream of Firebag
DS spill location	DownStream of spill location

LIST OF APPENDICES

CHAPTER 1 INTRODUCTION

With the development of human civilization, the human need to build structures and use consumables such as sand, bitumen, etc., has increased. As a result, different countries have been encouraged to extract oil from their sand sources, and the industry has been growing rapidly in recent decades. But the lack of sufficient river resources and the destructive environmental effects of extracting these resources have led governments to pay more attention to the resulting environmental impacts. These destructive environmental effects are not limited to the extraction site but are sometimes visible up to miles away from the extraction site. Extraction of Oil-Sands requires a large volume of water, which produces a significant amount of waste, which appears as suspended sediments from coarse-grained sand, fine-grained particles, and chemical contaminants (Dibike et al., 2018).

The largest source of oil sands in the world is in Canada and Alberta. The largest oil sands are located in the lower Athabasca River (LAR). The residual oil-sands mining processes are stored in some of the world's largest tailing storage facilities (tailing ponds) as shown in figure 1.1. In an event of a breach, these tailing ponds may cause a disastrous impact on the environment, public health, life, and property. Many historical catastrophic tailing breaches in Canada, e.g., Mount Polley tailing breach in British Columbia (2014) and around the world for example the Brumadinho dam disaster that occurred (2019) in Brazil, significant dam failures in Aitik in Sweden (2000), and Baia Mare in Romania (2000), have caused concerns about the risk of associated with oil-sands tailing ponds. Many studies have been conducted on the pollution of the tailings dams' failure in recent years. While, in this study, unlike previous studies, an attempt has been made to evaluate the downstream consequences of tailings release to the LAR (following hypothetical tailing pond failures), on the sediment transport and water quality regime for various scenarios, under changing climate.

The approach used in this study is to select the Mildred Lake Settling Basin (MLSB) tailings pond as a representative in the lower Athabasca oil sands area, and the effects of the release scenarios of the hypothetical tailings resulting from the sudden failure of the MLSB are investigated by a hydrodynamic model. The model selected in this study is The Environmental Fluid Dynamics Code (EFDC) model. A hydrodynamic model can model the hydrodynamic behavior and non-Newtonian aspect of flows resulting from the tailings dams' failure.

Figure 1.1 oil-sand tailing ponds (Canada)

This study is divided into two parts: In the first part, five tailings dam failure hypotheses were used for 30 days. In the second part, based on climate change data, five hypotheses of tailings dam failure for the future were simulated. This 30-day period allows the behavior of sediments to be examined during this time.

This dissertation has been prepared in 6 chapters. We begin by reviewing the literature on the failure of tailings dams in the world, then deal with the definitions in non-Newtonian numerical models. Chapter 3 summarizes the procedure. The fourth chapter is a submitted article that aims to simulate the hypothetical failure of a dam from oil-sands numerically. Chapter 5 is a general discussion of the results of previous chapters. Chapter 6 concludes with tips and insights for improving constraints.

CHAPTER 2 LITERATURE REVIEW

The literature on tailings dam failure in the world is reviewed in this chapter, then the non-Newtonian numerical model selected in this study is reviewed. Finally, we have an overview of future climate change research. In the first part, we first look at the nature of tailings dams and then review historical failures of tailings dams worldwide. In the second part of this chapter, an overview of the numerical models used in similar studies was given. Then the fine sediment transport model and the simulation of chemical constituents will discuss. This section has also tried to look at the rheological models used to model different flows (Newtonian and non-Newtonian fluids). In the end, climate change and the literature on the effects of climate change on tailings dams in the world are reviewed.

2.1 Tailing dams

Mines can consume very large amounts of water. These are especially true of processing units and related activities. It may also occur in activities such as dust prevention or other activities. Water is also lost due to evaporation in the final product, but most water loss is due to tailings flow. Tailing dams are structures (engineering or traditional) on the ground or underground to prevent the uncontrolled release of water, effluent, sludge, or solids on the ground or underground so that the intended materials can be emptied accumulated, and stored in it.

The bitumen extraction process produces a large volume of liquid useless that is spilled into the waste ponds. These materials consist of oily sand, debris consisting of solids (sand, clay, and silt particles), and contaminated OSPW[1] spilled into tailings ponds (Gosselinn et al., 2010). Most solids (<75%) in oil sand tailings are coarse solids that rapidly settle to the bottom of the pond (Dibike et al., 2018). After a few years, 30 to 35 % of fine solids settle and are called Mature Fine Tailings (MFT). Consolidation of MFT takes several years, and they remain in a fluid shape for several years or maybe decades. Coarse sands (MFT[2]) are often sediment to build tailings ponds dykes to contain fine liquid tailings (Gosselinn et al., 2010). After depositing MFT, fine fluid tailings (FFT)

[1] Oil Sands Process-affected Water

[2] Mature Fine Tailings

and Oil Sands Process-affected Water (OSPW) will form a tailings pond in the following. Ingredients in tailings ponds can vary (Allen, 2008). However, Figure 2.1 shows a schematic representation of a typical oil tailings pond.

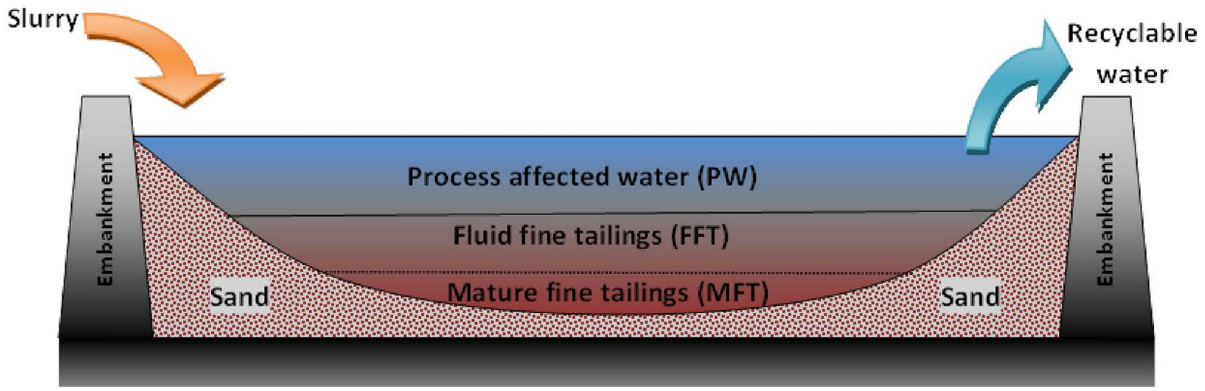

Figure 2.1 a schematic representation of a typical oil tailings pond (Dibike et al., 2018)

2.1.1 Chemical constituents of tailings storage facilities

Oil-sands are an unconventional source of oil. Bituminous sands are either found as loose sands or as hardened rocks from a mixture of water, sand, clay, and bitumen (very heavy oil with a much higher viscosity than ordinary oil). The province of Alberta in Canada has the third-largest oil reserves globally after Venezuela and Saudi Arabia. Of course, only Canada has a significant industry to extract bitumen sand. There are three major oil sand deposits in northern Alberta, including Athabasca, Cold Lake, and Peace River, covering approximately 140,200 km^2 (Dibike et al., 2018; Li et al., 2017). The world's largest bitumen sand deposit is located in Athabasca, northeast of Alberta, and its two extraction plants produce 73 million barrels of oil per year. About 14% of the sand in this area is extracted by light extraction methods, one of the world's largest operations. The sand is then washed with very hot water, and the tar is separated from it and converted into synthetic crude oil by adding hydrogen and performing other chemical processes. Thus, about 83% of the tar is converted into synthetic crude oil, and this extraction rate is much better than the amount obtained from many oil wells. The tar contains up to 5% sulfur, of which more than 98% is extracted during processing. It becomes. Although the volume of reserves in the

Athabasca bitumen sand may reach one trillion barrels, only a small amount of them, about 35 percent, can be extracted in a billion barrels with current methods. Nevertheless, it is estimated that by 2030, the production of bitumen by the oil sand industry in this region will achieve 3.95 million barrels per day (CAPP, 2015).

As mentioned, the petroleum sand industry produces large volumes of water under the influence of the bitumen extraction process. Heavy metals such as cobalt, nickel, lead, vanadium, cadmium, selenium, mercury, arsenic, copper, chromium, zinc, and iron naturally exist in oil sands be fixated by this process. Generally, the oil sands tailings combination contains almost 70 to 80 % water, 1 to 3 % bitumen, and 20 to 30 % solids (Kasperski 1992). The sequences contain water influenced by the sediment slurry containing contaminants and oil sands process affected water (OSPW) such as naphthenic acids (NA), polycyclic aromatic hydrocarbons (PAHs), phenols, heavy metals, and ions (van den Heuvel et al., 2012; Frank et al., 2014; Kavanagh et al., 2009; Allen, 2008).

The chemical composition of OSPW from tailings ponds in different mines can be different. But in general, OSPW produced from oil-sand mines is highly toxic to aquatic organisms. Due to the high toxicity of some substances such as naphthenic acids to aquatic creatures (Hadley et al., 2011), the oil sand industry will face environmental and operational challenges in the region (Stasik et al., 2014). Naphthenic acids (NAs) are the main constituent of tailings ponds and one of the main pollutants (MacKinnon and Boerger, 1986; Clemente and Fedorak, 2005; Dibike et al., 2018). The range of NAs concentrations varies between tailings ponds from 20-80 mg/L in fresh settling basins and 5-40 mg/L in experimental wetlands (Li et al., 2017; Mahaffey and Dube, 2017). Toxic effects of other substances in OSPW, such as PAHs, heavy metals, etc., have also shown a wide range of biological disorders in the body of the aquatic organism, such as mutagenicity, carcinogenicity, and immunotoxicity (Li et al., 2014). Dibike et al. (2018) and vanadium (V), more than the Canadian Council of Environment (CCME) water quality guidelines for aquatic life. They also name sodium, bicarbonate, chloride, and sulfate as other chemical compounds in the tailings pond. Table 2.1 clearly shows the chemistry of oil-sands process waters in the Athabasca River.

Table 2.1 the chemistry of oil sands process waters in the Athabasca River and regional lakes (Allen et al., 2008)

Variable (mg/L unless otherwise noted)	MLSB (2003)[a]	Syncrude demonstration ponds (1997)[b]	Suncor TPW (2000)[c]	Suncor CT release water (1996–97)[d]	Suncor CT Pond seepage (1996–97)[d]	Athabasca River (2001)[e]	Regional lakes (2001)[e]
COND ($\mu S.cm^{-1}$)	2400f	486–2283	1113–1160[f]	1700	1130	280	70–226
TDS	2221	400–1792	1887	1551	1164	170	80–190
Calcium	17	15-41	25	72	36	30	2-25
pH	8.2[g]	8.25–8.8	8.4	8.1	7.7	8.2	7–8.6
Sodium	659	99–608	520	363	254	16	<1–10
Ammonia	14[g]	0.03-0.16	14[f]	0.35	3.4	0.06	<0.05-0.57
Bicarbonate	775	219-667	950	470	780	115	9-133
Magnesium	8	9-22	12	15	15	8.5	1-8
Chloride	540	4-258	80	52	18	6	<1-2
Sulfate	218	70-513	290	564	50	22	1-6

Note: MLSB, Mildred Lake Settling Basin; CT, consolidated tailings; TPW, tailings pond water; COND, conductivity TDS, total dissolved solids; ranges indicate mean values for multiple sites; data represent mean values from samples collected during the year indicated.

[a](MacKinnon 2004).

[b](Siwik et al. 2000).

[c](Kasperski 2001).

[d](Farrell et al. 2004).

[e](Golder Associates Limited 2002).

[f](MacKinnon and Sethi 1993).

[g](MacKinnon 2001).

Hadley et al. 2001 used various environmental samples collected over three years from selected tributaries of the Athabasca River Basin. After evaluating polycyclic aromatic hydrocarbons (PAHs) and their alkylated analogs, they concluded that samples from petroleum sand deposits included the highest quantity of PAHs and alkylated PAHs. Total PAH levels also increased in tributaries such as the Ells River, Steepbank River, and MacKay River compared to the main stem of the Athabasca River. Some studies also examined the spatial patterns of natural PAH deposition in the LAR (Akre et al., 2004; Timoney and Lee, 2009; Wiklund et al., 2014; Shakibaeinia et al., 2017). Shakibaeinia et al. 2017 used a hydrodynamic model to investigate the transport of well-cohesive sediments and related chemical compounds in the cold zone. The simulation results showed that the concentration of chemical compounds is higher only near the junction and gradually decreases with the downstream distance from the junction. In general, many studies have been conducted that show that tailings ponds contain large concentrations of toxicological metals that can be referred to for further studies(such as Siwik et al., 2000 and McQueen et al., 2017).

2.1.2 Tailings dams failures

Tailings dams are always likely to fail for reasons such as leaks, foundation failure, steep slopes, and earthquakes. As a result, a significant amount of waste is discharged into the natural environment and will cause heavy losses, and serious economic and environmental damage. In recent years, tailings dam failure has not been uncommon in developing countries, for example, the failure of the tailings dam in Brazil (2015) or a similar environmental disaster in the US in the same year. In that environmental disaster, about 11.5 million liters of water collected behind the mineral tailings stored in this area entered the "Animas" river. Following this incident, toxic waste contaminated hundreds of kilometers of the river, and the water turned completely orange.

There have been other similar occurred around the world, of which Canada is no exception. For example, the tailings dam breach in Mount Polly (2014, British Columbia), Mount Obed (2013, Alberta), and Galbridge (2012, Newfoundland). The closest failure in Canadian history was in Mount Polly. This incident happened on August 4, 2014, and eight million cubic meters of tailings into Hazeltine Creek, Quesnel Lake, and Polley Lake figure 2.2.

Figure 2.2 satellite image of Mount Polly before (left image) and after (right image) the tailings dam breach (Mahdi et al., 2020)

2.2 Contaminant transport modeling

The governing transport equations for pollutant transport can be formulated for transport in three dimensions. But in general, the formula of one-dimensional modeling is simpler and can be used in many practical environmental problems, and at the same time, it can be said that two- and three-dimensional modeling have higher accuracy, and according to possible achievements and goals, the ability different of them will be considered.

The pollutants in water transfer in the form of suspended or dissolved particles in surface or underground water. In surface water, particles enter streams and rivers and move downstream in the form of particles by rolling, sliding, and desalination, and are mostly deposited downstream. Also, this transfer depends on flow speed, turbulence, grain size, shape, and density (Rubin, 2005). This part presents processes related to toxins and their mathematical modeling (Basic equations and numerical aspects).

For the part of the pollutant that dissolves directly in the water phase, the basic equation (1) is used (EFDC+ Theory, 2020):

$$\frac{\partial}{\partial t}(mHC_w) + \frac{\partial}{\partial x}\left(m_y H_u C_w\right) + \frac{\partial}{\partial y}(m_x H_v C_w) + \frac{\partial}{\partial z}(m_w C_w) = \frac{\partial}{\partial z}\left(m\frac{A_b}{H}\partial_z C_w\right) +$$
$$mH(\sum_i\left(K_{dS}^i S^i \partial_S^i\right) + \sum_j\left(K_{dD}^j D^j \partial_D^j\right)) - mH\left(\sum_i K_{as}^i S^i\right)(\partial_w \frac{C_w}{\partial})(\hat{\partial}_S^i - \partial_S^i) -$$
$$mH\left(\sum_j K_{aD}^j S^j\right)(\partial_w \frac{C_w}{\partial})(\hat{\partial}_D^j - \partial_D^j) + S_C^E + S_C^I \quad (1)$$

where,

S^i: The sediment mass, class i (g/m^3),

C_w: The water dissolved contaminant mass per unit total volume (µg/l),

D^j: The dissolved substance mass (g/m^3),

X_D: The contaminant absorbed mass to dissolved material j per unit mass of dissolved material (mg/g),

X_S: The contaminant absorbed mass to sediment class i per sediment mass (mg/g),

ø: The porosity (dimensionless),

Ψ_W: The water dissolved contaminant available fraction for absorption (dimensionless),

K_a: The absorption rate of sediment (S) or dissolved material (D) (/s),

S_C^I: The internal source/sink of the contaminant (mg/s) due to degradation, volatilization, and conversions to/from other contaminants (mg/s),

S_C^E: The external source/sink of the contaminant (mg/s), and

K_d: The deabsorption rate (/s).

In the water column, the transport of an absorptive contaminant is governed by transport equations. Therefore, the transport equations for the pollutant dissolved in the water phase, for the pollutant adsorbed to the effectively dissolved substance in the water phase, and for the pollutant adsorbed to suspended particles govern.

The summary of equations governing the transformation process and distribution is presented in the form of differential equations (2) to (6) (Shakibaeinia et al., 2017).

Dissolved chemical in the water column:

$$\frac{\partial D_w}{\partial t} = \overbrace{-K_w K_{dw} D_w C}^{\text{adsorption}} + \underbrace{K_w A_w}_{\text{desorption}} + \varepsilon \frac{\overbrace{(D_S/(\eta dz_S) - D_w)}^{\text{diffusion}}}{(dz_f + dz_S)dz} - \underbrace{d_B + d_H + d_P}_{\text{degredation}} + \overbrace{K_{ev} D_w / dz}^{\text{evaporation}} \quad (2)$$

Adsorbed chemical in the water column:

$$\frac{\partial A_w}{\partial t} = \overbrace{K_w K_{dw} D_w C}^{\text{adsorption}} - \underbrace{K_w A_w}_{\text{desorption}} - \overbrace{W_S A_w / dz}^{\text{sediment}} + \underbrace{R_S/(M_S dz)}_{\text{resuspension}} \quad (3)$$

Dissolved chemical in bed sediments:

$$\frac{\partial D_S}{\partial t} = -\overbrace{K_S K_{dS} D_S M_S/(ndZ_S)}^{\text{adsorption}} + \underbrace{K_S A_S}_{\text{desorption}} + \varepsilon \frac{\overbrace{(D_w/(\eta dz_S) - D_w)}^{\text{diffusion}}}{(dz_f + dz_S)} - \underbrace{d_B + d_H}_{\text{degredation}} \quad (4)$$

Adsorbed chemical in bed sediment:

$$\frac{\partial A_S}{\partial t} = -\overbrace{K_S K_{dS} D_S M_S/(ndZ_S)}^{\text{adsorption}} - \underbrace{K_S A_S}_{\text{desorption}} + \overbrace{W_S A_w/dz}^{\text{sediment}} - \underbrace{R_S A_S/(M_S dz)}_{\text{resuspension}} \quad (5)$$

Total Sediment Suspended (TSS):

$$\frac{\partial c}{\partial t} = \overbrace{W_S c/dz}^{\text{sediment}} - \underbrace{R_S/dz}_{\text{resuspension}} + \overbrace{R_P/dz}^{\text{production}} \quad (6)$$

Where K_{ds} and K_{dw} are the coefficients of the partitioning in the bed sediments and water column, respectively, k_w and k_s are the rates of desorption in the water column and bed sediment, respectively, R_p is the rate of particle production, R_s is the suspension rate of sediments, η is the

porosity, M_S is the sediments mass, dz_f, dz_s, dz are computational grid, water film, sediment layer thicknesses, respectively, d_P, d_B, and d_H account for photolysis, hydrolysis, and bio-decay, respectively, k_{ev} is the evaporation rate, ε is the diffusion coefficient, W_s is the velocity of sediment settling.

2.3 Sediment Transport Processes

Hydrodynamics should be considered the science of studying moving fluids by analytical and mathematical methods. Hydrodynamic modeling for showing the dynamics of moving fluids is efficient. These numerical computational models can simulate flows, water levels, sediment transport, salinity, water quality, etc. With the breach of the dam, the behavior pattern of the flow in the river will change. These changes affect the hydraulic conditions of the flow in the river. Numerical models have particular importance in changing flow parameters and lower costs than physical models due to accurate calculations and flexibility. However, understanding the structure and application of the models can help achieve any research on the purpose of the project.

2.3.1 Sediment Transport Modeling

The first step in numerical simulation is to select the appropriate numerical model for the problem. There are numerous mathematical models for simulating sediment transport in one-dimension (1D), two-dimension (2D), and three-dimension (3D) (Martin and McCutcheon, 1999; Chaudhry, 1993).

2.3.1.1 One Dimensional (1D) Models

In most studies of river system models in which it can be assumed that the effect of water layers on each other can be neglected, a one-dimensional system is used to model the flow. In this case, the equations of momentum and continuity, commonly known Saint-Venant equations, can be used. These equations are used in these models as follows:

$$\frac{\partial Q}{\partial x}\Delta x + T_W \frac{\partial Z}{\partial t}\Delta x = Q_L \qquad (7)$$

where,

Q=Q (x,t)= flow rate,

A= A (x,t)= Flow cross-section area,

Q_L=Q_L (x,t)= Input or output lateral flow, negative for outflow and positive for inflow,

Z= Z (x,t)= Water level elevation= H (x,t)+Z_b (x),

H (x,t)= flow depth,

T_w=T_w (x,t)= flow top width.

The momentum equation is also written as follows:

$$\frac{\partial Q}{\partial t} + \beta \frac{\partial (\frac{Q^2}{A})}{\partial x} = -gAS_f - gA\frac{\partial Z}{\partial x} \quad (8)$$

S_f = S_f (x,t) is the energy line slope and is defined as follows using the Manning or Chézy relation:

$$S_f = \frac{n^2U^2}{R^{4/3}} = \frac{U^2}{RC^2} = \frac{Q|Q|}{C^2A^2R} \quad (9)$$

where,

C (x,t): Chezy coefficient factor,

R (x,t) : Hydraulic flow radius.

The terms in equation (8), from left to right, are; 1) local acceleration, 2) displacement acceleration, 3) bed resistance, and 4) pressure gradient. By substituting Equation (9) in equation (8), Expanding Term 2 of equation (8), and replacing $\frac{\partial Q}{\partial x}$ With equation (7), the momentum equation is written as follows.

$$\frac{\partial Q}{\partial t} + \frac{2\beta Q Q_L}{A\partial x} - \frac{2\beta Q T_w}{A}\frac{\partial Z}{\partial t} - \frac{\beta Q^2}{A^2}\frac{\partial A}{\partial x} = -gA\frac{\partial Z}{\partial x} - g\frac{Q|Q|}{C^2RA} \quad (10)$$

One of the main advantages of one-dimensional models is the simulation with the least amount of data. However, the 1D flow hypothesis may not be reliable in many cases, for example, flow in a channel along different cross-sections, complex tidal flows, or alignment. These models simulate the flow and deposition of sediment in the longitudinal direction without solving the cross-sectional details (Mashriqui, 2003). In other words, these models may achieve good outcomes when applied in channels with minimal change and limited hydraulic complexity in channel geometry in the streamwise direction (Johnson, 2008). According to the project objectives, these models have been used in many studies (Cunge et al., 1980; De Vries et al., 1989; Wu et al, 2000; Langendoen & Alonso, 2008). Some current one-dimensional models are shown in table 2.2.

2.3.1.2 Two Dimensional (2D) Models

2D sedimentary models are more complex, take longer to run, and require considerably more data input than 1D models. But other advantages of these models such as simulation of complex flow situations, more accurate hydrodynamic calculations (Papanicolaou et al., 2008), use of structured networks, simulation of lateral flow vector (Wu, 2008), and combination of turbulence through Ignored the coefficients of eddy viscosity with mean depth (Johnson, 2008). These models are according to motion equations and integrated depth continuity, and these models allow the simulation of the lateral flow vector (Wu, 2008; Johnson, 2008; Papanicolaou et al., 2008; Mashriqui, 2003). Table 2.3 lists several 2D sediment models and has compared several of their characteristics.

Zorkeflee (2004) studied the two-dimensional mathematical model CCHE2D and the one-dimensional model HEC-RAS in the Muda River. It was then concluded that although one-dimensional models such as HEC-RAS are widely used, they cannot analyze some of the hydraulic characteristics of the flow, such as flow and sediment patterns at windings and the range of structures and obstacles in the river. Mahdi et al. (2020) used a two-dimensional model, FLO-2D (O'Brien and Julien, 2000), to simulate a flood in the Athabasca River. FLO 2D uses a finite difference algorithm to solve the Saint-Venant equations (which contain momentum conservation and continuity). TABS-MD (Thomas and McAnally, 1990) and MIKE 21 (DHI, 2003) are popular and used in engineering practice (Mashriqui, 2003).

Table 2.2 a summary of one-dimensional models for sediment transport (Papanicolaou et al., 2008)

Model and references	Last Update	flow	Bed sediment transport	Suspended sediment transport	Sediment mixtures	Cohesive sediment	Sediment exchange processes	Executable	Source code	Language
FLUVIAL 11; Chang (1984)	-	Unsteady	Yes	Yes	Yes	No	Entrainment and deposition	C	P	FIV
HEC-6: Hydraulic Engineering Center; Thomas and Prashum (1977)	V. 4.2 (2004)	Steady	Yes	Yes	Yes	No	Entrainment and deposition	PD	PD	F77
MOBED: Mobile BED; Krishnappan (1981)	-	Unsteady	Yes	Yes	Yes	No	Entrainment and deposition	C	C	F90
IALLUVIAL: Iowa ALLUVIAL; Karim and Kennedy (1982)	-	Quasi-stead	Yes	Yes	Yes	No	Entrainment and deposition	C	C	FIV
CHARIMA: Acronym of the word CHARiage which means bedload in French Holley et al. (1990)	-	Unsteady	Yes	Yes	Yes	Yes	Entrainment and deposition	C	C	F77
GSTARS: Generalized sediment transport models for alluvial River simulation (Molinas and Yang, 1986)	V. 3 (2002)	Unsteady	Yes	Yes	Yes	No	Entrainment and deposition	PD	PD	F90/F95
SEDICOUP: SEDIment COUPled; Holly and Rahauel (1990)	-	Unsteady	Yes	Yes	Yes	No	Entrainment and deposition	C	C	F77
3STD1, steep stream sediment Transport 1D model; Papanicolaou et al. (2004)	-	Unsteady	[a]Yes	[a]Yes	Yes	No	Entrainment and deposition	C	P	F90
EFDC1D: Environmental fluid dynamics code; Hamrick (2001)	-	Unsteady	Yes	Yes	Yes	Yes	Entrainment and deposition	PD	PD	F77
OTIS: One-dimensional transport with inflow and storage; Runkel and Broshears (1991)	V. OTIS-P (1998)	Unsteady	No	Yes	No	No	Advection-diffusion	PD	PD	F77

Note: V=Version; C=copyright; LD=limitied distribution; P=proprietary; PD=public domain; and F=FORTRAN.

[a]Treated as a total load without separation

According to the governing equations, the two-dimensional equations of momentum conservation and depth-averaged mass are given below (Johnson, 2008).

$$\frac{\partial h}{\partial t}+\frac{\partial hu}{\partial x}+\frac{\partial hv}{\partial y}=0 \tag{11}$$

$$\frac{\partial u}{\partial t}+u\frac{\partial u}{\partial x}+v\frac{\partial u}{\partial y}+g\frac{\partial n}{\partial x}=\frac{1}{\rho h}\frac{\partial h\tau_{xx}}{\partial x}+\frac{1}{\rho h}\frac{\partial h\tau_{xy}}{\partial x}-\frac{\tau_{bx}}{\rho h}+f_{cor}v \tag{12}$$

$$\frac{\partial v}{\partial t}+u\frac{\partial v}{\partial x}+v\frac{\partial v}{\partial y}+g\frac{\partial n}{\partial x}=\frac{1}{\rho h}\frac{\partial h\tau_{yx}}{\partial x}+\frac{1}{\rho h}\frac{\partial h\tau_{yy}}{\partial x}-\frac{\tau_{by}}{\rho h}+f_{cor}u \tag{13}$$

where,

u = Longitudinal velocity component,

h = Depth of flow,

x = Spatial coordinate in the longitudinal direction,

v = Transverse velocity component,

t = Time,

y = Spatial coordinate transverse direction,

ρ = Density of water,

g = Gravitational acceleration,

n = Water surface elevation,

τ_{xy} and τ_{yx} = Shear stresses in the longitudinal and transverse directions,

τ_{bx} and τ_{by} = Bed shear stresses in the longitudinal and transverse directions,

τ_{yy} = Normal and turbulent stresses in the transverse direction

τ_{xx} = Normal and turbulent stresses in the longitudinal direction, and

f_{cor} = Coriolis parameter.

Then we will have the Reynolds stresses that are based on Boussineq's assumption:

$$\tau_{xx} = 2v_t \frac{\partial u}{\partial x} \quad (14)$$

$$\frac{\partial Q}{\partial t} + \beta \frac{\partial (\frac{Q^2}{A})}{\partial x} = -gAS_f - gA\frac{\partial Z}{\partial x} \quad (15)$$

$$\frac{\partial Q}{\partial t} + \beta \frac{\partial (\frac{Q^2}{A})}{\partial x} = -gAS_f - gA\frac{\partial Z}{\partial x} \quad (16)$$

where,

v_t = Eddy viscosity.

2.3.1.3 Three Dimensional (3-D) Models

3D models are more complex than other models, considering both vertical and horizontal components of sediment transport processes (Wu, 2008; Formann et al., 2007) and require more complete data and more time and cost. These models require complete field data, especially for calibration. Three-dimensional models can be a good choice for the full three-dimensional nature of the flow (Wu, 2008; Formann et al., 2007), with secondary and rotational flows, curved and irregular boundaries, complex topography, and changeable sediment transport. These models can more accurately apply the effect of 3D flow field simulation potential in calculations and bed shear stress. Some three-dimensional models are mentioned in Table 2.4 (Papanicolau et al., 2008).

Table 2.3 a summary of two-dimensional sediment transport models (Papanicolaou et al., 2008)

Model and references	Last Update	flow	Bed sediment transport	Suspended sediment transport	Sediment mixtures	Cohesive sediment	Sediment exchange processes	Executable	Source code	Language
TABS-2; Thomas and McAnnally (1985)	-	unsteady	[a]Yes	[a]Yes	No	Yes	Entrainment and deposition	C	C	F77
ADCIRC: Advanced CIRCulation; Luettich et al. (1992)	-	Unsteady	[a]Yes	[a]Yes	No	Yes	Advection-diffusion	C/LD	C/LD	F90
MOBED2: Mobile BED; Spasojevic and Holly (1990a)	-	Unsteady	Yes	Yes	Yes	No	Entrainment and deposition	C	C	F77
MIKE 21: Danish acronym of the word microcumputer; Danish Hydraulic Institute (1993)	-	Unsteady	[a]Yes	[a]Yes	No	Yes	Entrainment and deposition	C	P	F90
Transport models for Alluvial Rivers Simulations; Lee et al. (1997)	-	Unsteady	YES	Yes	YES	No	Advection-diffusion	PD/C	P	F90
UNIBEST- TC: UNIform Beach Sediment Transport - Transport Crossshore; Bosboom et al. (1997)	-	Quasi-steady	[a]Yes	[a]Yes	NO	No	Entrainment and deposition	C	LD	F90
FAST2D: Flow Analysis Simulation Tool; Minh Duc et al. (1998)	-	Unsteady	Yes	Yes	No	No	Entrainment and deposition	LD	P	F90
CCHE2D: The National Center for Computational Hydroscience and Engineering; Jia and Wang (1999)	V. 2.1 (2001)	Unsteady	Yes	Yes	Yes	No	Advection-diffusion	PD/C	LD	F77/F90
Delft 2D; Walstra et al. (1998)	-	Unsteady	Yes	Yes	No	Yes	Advection-diffusion	C	LD	F90
FLUVIAL 12; Chang (1998)	-	Unsteady	Yes	Yes	Yes	No	Entrainment and deposition	C	P	F77

Note: V=Version; C=copyright; LD=limitied distribution; P=proprietary; PD=public domain; and F=FORTRAN.

[a]Treated as a total load without separation

In 3D models is used the convection-diffusion equations or the three-dimensional mass balance equations are for suspended sediment transport. Current governing equations The Navier-Stokes time-averaged equations are known as the Reynolds equations (RANS). The general form of these equations, which includes a continuity equation and three momentum equations in three directions, is as follows:

$$\frac{\partial \rho}{\partial t} + \frac{\partial (\rho u_i)}{\partial x_i} = 0 \tag{17}$$

$$\frac{\partial Q}{\partial t} + \beta \frac{\partial (\frac{Q^2}{A})}{\partial x} = -gAS_f - gA\frac{\partial Z}{\partial x} \tag{18}$$

where,

u_i: Flow velocity in the direction of the x_i axis,

ρ: Fluid density,

β_i: Volumetric forces,

μ: Dynamic viscosity, and

μ_t: Turbulence viscosity.

Suppose we want to make a general conclusion in this section. In that case, it should be said that in recent decades, the use of numerical models that analyze the flow in rivers by solving the main equations has become very common. With the increasing power of computers, numerical models have also been expanded. In simple conditions, one-dimensional numerical models can be used and sediment transport calculations to predict water leaching and sedimentation (Wong and Prker, 2006). In more complex terms, the application of two-dimensional models averaged at depth and three-dimensional models assuming hydrostatic pressure to solve equations is justified in shallow water where secondary flows and turbulence fluctuations are not severe (Kuipers and Vreugdenhil, 1973).

One of the models that have been widely used in the last few decades is the Environmental Fluid Dynamics Code (EFDC). EFDC is a state-of-the-art hydrodynamic model, and it can use in one,

two, and three dimensions. Figure 2.3 shows how the transfer module works in EEMS the sediment transport model combined with the hydrodynamic simulation model. The sediment transfer model will calculate the sediment transport behaviors in the sediment bed and the water column.

Table 2.4 a summary of two-dimensional sediment transport models (Papanicolaou et al., 2008)

Model and references	Last Update	flow	Bed sediment transport	Suspended sediment transport	Sediment mixtures	Cohesive sediment	Sediment exchange processes	Executable	Source code	Language
ECOMSED: Estuarine, Coastal, and Ocean Model - SEDiment Transport; Blumber and Mellor (1987)	V. 1.3 (2002)	Unsteady	[a]Yes	[a]Yes	No	Yes	Entrainment and deposition	PD	PD	F77
RMA-10: Resource Management Associates; King (1988)	-	Unsteady	[a]Yes	[a]Yes	No	Yes	Advectiondiffusion	C	P	F77
GBTOXe: Green Bay TOXic enhancement; Bierman er al. (1992)	-	unsteady	No	Yes	No	Yes	Entrainment and deposition	NA	NA	F77
EFDC3D: Environmental Fluid Dynamics code; Hamrick (1992)	-	Unsteady	Yes	Yes	Yes	Yes	Entrainment and deposition	PD	P	F77
CH3D-SED: Computational Hydrauilcs 3DSEDiment; Spasojevic and Holly (1994)	-	Unsteady	Yes	Yes	Yes	Yes	Entrainment and deposition	C	C	F90
ROMS: Regional Ocean Modeling System; Song and Haidvogel (1994)	V. 1.7.2 (2002)	Unsteady	Yes	Yes	Yes	No	Entrainment and deposition	LD	LD	F77
FAST3D: Flow Analysis Simulation Tool; Landsberg et al. (1998)	V. Beta-1.1 (1998)	Unsteady	Yes	Yes	No	No	Entrainment and deposition	LD	P	F90
SSIIM: Sediment Simulation In Intakes with Multiblock options; Olsen (1994)	V. 2.0 (2006)	Unsteady	Yes	Yes	Yes	No	Advection-diffusion	PD	P	C-Langua.
TELEMAC; Hervouet and Bates (2000)	-	Unsteady	[a]Yes	[a]Yes	No	Yes	Entrainment and deposition	C	P	F90
MIKE 3: Danish acronym of the word Microcomputer; Jacobsen and Rasmussen (1997)	-	Unsteady	[a]Yes	[a]Yes	No	Yes	Entrainment and deposition	C	P	F90
Zeng et al. (2005)	V. 2.1 (2001)	Unsteady	Yes	Yes	No	No	Entrainment and deposition	P	P	F90
Delft 3D; Delft Hydraulics (1999)	V.3.25.00 (2005)	Unsteady	Yes	Yes	No	Yes	Entrainment and deposition	C	LD	F77

Note: V=Version; C=copyright; LD=limitied distribution; P=proprietary; PD=public domain; and F=FORTRAN.

[a]Treated as a total load without separation

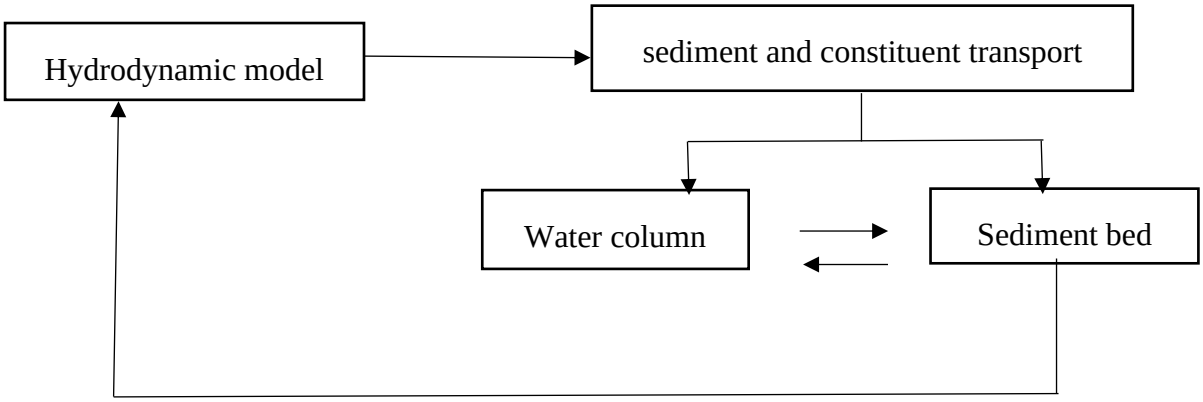

Figure 2.3 transfer module in the hydrodynamic model

2.3.2 Geomorphological Modeling

Geomorphological conceptual models are the conceptual model's category. These models are based on the deposition of sediments at the mouth of the river on field observations or experiments (Mashriqui, 2003). These models have been used to study rivers worldwide, such as the Mississippi River in the United States, the Atchafalaya River in Louisiana, and the Jamuna River in Bangladesh (Mashriqui, 2003; Ashworth et al., 2000; Heerden, 1980; Welder, 1959).

2.3.3 Physical Modeling

Physical models are often computationally difficult to simulate, and their uncertainty depends to a great extent on the quality and quantity of the data measured. Physical models incorporate the appropriate equations governing processes without simplification. (Dalrymple, 1985). Analyzing flows in rivers often uses semi-empirical equations resulting from field investigation and laboratory studies and thus has an enormous approximation. The high cost of physical models, non-generalizable results, limited use of measuring devices, and time-consuming also limit the use of these models.

In general, each model can be selected according to the conditions in the area, available data, project objective, and many other influential cases and can be used according to the type of event.

Choosing a model to simulate an event is an important element in achieving the correct and desirable results.

2.4 Numerical models

A range of flows in nature is of different phases. The physical phases of these flows include gas, liquid, and solid. Advances in computational fluid mechanics have provided a foundation for more insight into the dynamics of multiphase flows. Numerical models have been developed for many years to estimate and interpret results such as flow velocity, water depth, and flow pressure. Based on this, hydrodynamic problems can be analyzed by Eulerian, Lagrangian methods, or a combination of the two. The choice of each three methods for problem analysis depends on the characteristics and nature of the problem.

2.4.1 Eulerian and Lagrangian methods

Eulerian's theory applies to most engineering problems, and it can be used more easily in fluid analysis. In Eulerian's theory, analysis of steady-state flows is easy, so in unstable flow, the variables (properties) of the fluid will change with time in the spatial points of the flow. In contrast, in the steady stream, none of the variables at the points change with time. Due to the strong connection effect between continuous and scattered phases, The Eulerian multiphase model is the most advanced multiphase flow model.

The phase-average continuity and momentum equations for the phase «k»:

$$\frac{\partial}{\partial t}(\bar{\alpha}_k \rho_k) + \nabla\left(\bar{\alpha}_k \rho_k \widetilde{U}_k\right) = 0 \tag{19}$$

$$\frac{\partial}{\partial t}\left(\bar{\alpha}_k \rho_k \widetilde{U}_k\right) + \nabla\left(\bar{\alpha}_k \rho_k \widetilde{U}_k \times \widetilde{U}_k\right) = -(\bar{\alpha}_k \nabla \tilde{\rho}) + \nabla \check{\tau}_k^t + [F_{DC} + F_{VM} + F_L] \tag{1}$$

$$F_{DC} = K_{dc}\left[\left(\widetilde{U}_d - \widetilde{U}_c\right) - \left\{\frac{\overline{\alpha_d \acute{U}_d}}{\alpha_d} - \frac{\overline{\alpha_c \acute{U}_c}}{\alpha_c}\right\}\right] \tag{21}$$

$$F_{VM} = 0.5\alpha_p \rho_p \left(\frac{d_q \overline{v_q}}{dt} - \frac{d_p \overline{v_p}}{dt}\right) \tag{22}$$

where,

P: Pressure,

T: Time,

V: Volume,

p, q: Primary and secondary phase respectively,

α: Volume fraction (dimensionless),

τ_{ij}: Surface stress tensor,

τ_q: Phase stress-strain tensor (Pa),

K_{dc}: Drag Coefficient,

U: Velocity (ms^{-1})

F_{DC}, $F_{VM,}$ and F_L: The drag, virtual mass, and lift forces, respectively.

Newtonian and non-Newtonian flows are discussed in analyzing currents resulting from the sudden breaking of tailings dams. For this reason, the use of Eulerian and Lagrangian models in such modeling will be important. For example, the Eulerian multiphase model in ANSYS FLUENT allows us to perform multiple modeling separately with the interacting phases. Phases can be gasses, solids, or liquids in almost any composition. An Eulerian view is applied for each phase instead of the Eulerian-Lagrangian view used for the distinct phase model. The Eulerian model in ANSYS FLUENT does not distinguish between liquid-liquid and liquid-solid (granules) in multiphase flows. Granular flow is a flow that has at least one granule phase. The FLO-2D model also simulates non-Newtonian currents by solving St. Venet equations and by the rheological representation of the quadratic model. Several studies have been used to simulate this type of flow under the influence of flooding or dam failure. For example, Mahdi et al. (2020) performed numerical simulations of runoff and non-Newtonian ground currents to investigate hypotheses of sub-tailings dam violations in sand oil fields. In this study, they used the FLO-2D model, which is a rheological model.

But it must be borne in mind that solving Eulerian equations is not always possible in some cases due to complexity, such as the Navier-Stokes equations. Among the methods that use Eulerian's

view is simulation through the numerical solution to finite element, finite volume, and finite difference methods. The quantities of flow must be determined on the nodes. The Eulerian model is approximately similar to the Lagrangian model. One of the main practical problems of this method is that its analysis is a very complex and difficult task despite the simple form of the equations. Also, the continuity of the flow does not make the problem easier because the particle in its path may change. This method is more applicable in one-dimensional flows.

The governing equations for fluid flow used in EFDC+ are the advection-diffusion equations and Navier-Stokes for dye, toxic substances, salinity, suspended sediment transport, and temperature (DSI, 2020). In this model for mass transport, the advection-diffusion equation in a three-dimensional curvilinear orthogonal coordinate system is as follows (Hamrick and Wu, 1997; Hamrick, 1992, 1996):

$$\frac{\partial C}{\partial t}+\frac{\partial (uC)}{\partial x}+\frac{\partial (vC)}{\partial y}+\frac{\partial (wC)}{\partial Z}=\frac{\partial}{\partial x}\left(A_H\frac{\partial C}{\partial x}\right)+\frac{\partial}{\partial y}\left(A_H\frac{\partial C}{\partial y}\right)+\frac{\partial}{\partial z}\left(A_H\frac{\partial C}{\partial z}\right) \quad (23)$$

where,

t: time,

A_H and A_b: the horizontal and vertical diffusion coefficients, respectively,

(*u;v;w*): velocity components of fluid flow,

C: concentration, and

(x;y; z): Lagrangian coordinates of a particle.

Lagrangian differential equations of particle motion correspond to equation (17) and are as follows:

$$d_x=\left(u+\frac{\partial A_H}{\partial x}\right)dt+(2p-1)\sqrt{2A_H dt} \quad (24)$$

$$d_y=\left(u+\frac{\partial A_H}{\partial y}\right)dt+(2p-1)\sqrt{2A_H dt} \quad (25)$$

$$d_z=\left(u+\frac{\partial A_H}{\partial z}\right)dt+(2p-1)\sqrt{2A_H dt} \quad (26)$$

where,

p: A random number from a uniformly distributed random variable generator with a mean 0.5, and

d_t: The time step.

2.5 Climate change

Climate change is a significant change in the average meteorological data over a period of time. This period is usually ten years or more (Mander, 1994). At present, climate change has disrupted the Earth's hydrological cycle, especially its temporal and spatial distribution. So it is important to investigate and predict its changes because they can significantly impact ecosystem dynamics like water level changes and flow rate.

Temperature and precipitation are two important variables in determining the climate of a region, and changes in these two variables, directly and indirectly, affect different systems. Therefore, these changes can directly affect the natural inflows in a basin by predicting global warming and affecting the amount of future rainfall and, of course, the direct impact on the storage volume and discharge in the basin. Hydrological studies use general physical climate models, as shown in figure 2.4. These models (AOGCM, GCM, SDM, RCM, and EBM) are reviewed under different scenarios.

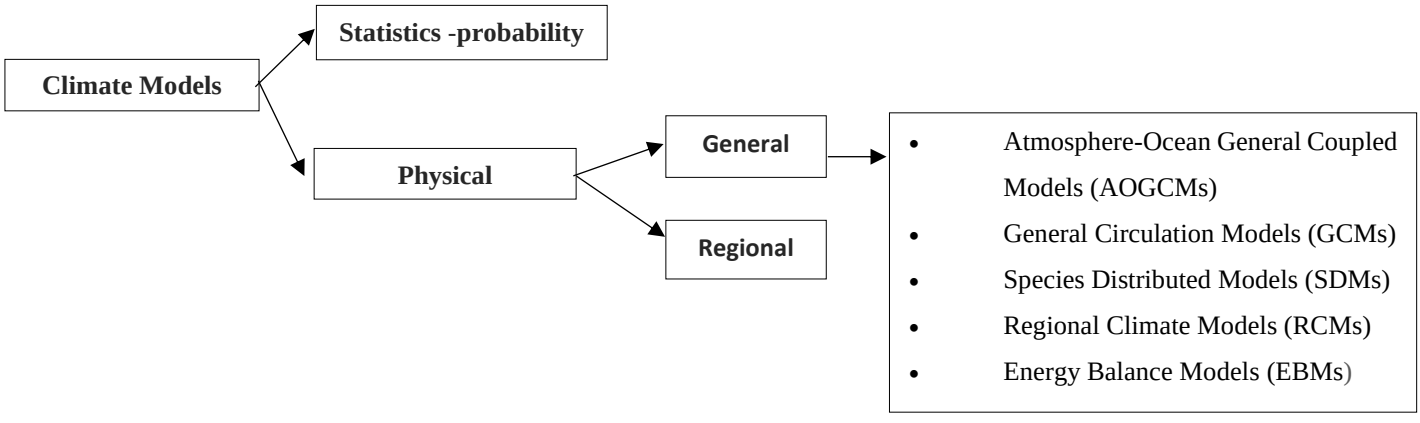

Figure 2.4 a variety of climate models

2.5.1 Climate models

According to climate models, global warming has increased the probability of increasing the rainfall event intensity and following the change in rainfall (Trenberth et al., 2007). In some hydrological studies, Atmosphere-Ocean General Coupled Models (AOGCMs) have shown that the uncertainty caused by the AOGCM models has been more significant than the hydrological models (Teng et al. 2012; Prudhomme and Davies 2009), So it can be said that these models have a high degree of uncertainty. But on the other hand, General Circulation Models (GCMs) and Regional Climate Models (RCMs) are commonly used to determine the hydrological effects of climate change in different regions.

RCM is the same as the GCM pattern restricted to a subset of the global pattern network and dynamically uses temporal changes in atmospheric conditions based on the GCM pattern. Both models have a significant effect on determining climate change due to increased greenhouse gas emissions. Most regional climate models derived from general circulation models cannot show future variables. Although most GCMs widely represent the general trend, there are still uncertainties in quantity, variability, and especially local patterns, which should be considered in future studies.

2.5.2 An introduction to the new series of emission scenarios called RCPs

The RCPs scenarios were proposed in 2010 by a scientific committee under the supervision of the Intergovernmental Panel on Climate Change (IPCC). These scenarios aim to provide a set of information from the results of which the main factors of climate change can be traced and the results can be applied to climate models. The Representative Concentration Pathway (RCP) family scenarios include 4 different scenarios, which are: 8.5, 6, 4.5, and 2.6, which are based on different specifications of the social and economic situation, technology level, and policies in the future, which are in each situation. It can lead to different emission levels of greenhouse gases and climate change.

In the RCP6 scenario, the CO_2 concentration is estimated at 850 PPM until the year 2100, and the effect of greenhouse gases on radiative forcing is estimated at up to 6 W/m^2. In the RCP8.5 scenario, the CO_2 concentration is estimated at 1370 PPM until the year 2100, and the effect of greenhouse gases on radiative forcing is estimated to be 5.8 W/m^2. In the RCP2.6 scenario, the

CO_2 concentration is estimated at 490 PPM until the year 2100, and the effect of greenhouse gases on radiative forcing is estimated at up 6.2 W/m^2. In the RCP4.5 scenario, the CO_2 concentration is estimated at 650 PPM until the year 2100, and the effect of greenhouse gases on radiative forcing is estimated at 5.4 W/m^2 (Vuuren et al., 2011a; Vuuren et al., 2011b; Riahi et al., 2011).

The variables of this scenario are:

The concentration of aerosols and active chemical gases (O_3, aerosol).

Some gas emissions: CFCs, CO_2, HFCs, CH4, PFCs, and SF_6.

The concentration of greenhouse gases such as CH_4, CO_2, HFCs, CFCs, PFCs, SF_6, and, N_2O.

The emission rate of active chemical gases and aerosols, organic carbon, black carbon, VOCs, SO_2, CO, NH_3, and NOx.

Land user data and land surface cover.

Investigations by the Intergovernmental Panel on Climate Change (IPCC) in the fifth report as the latest climate change report showed that based on the RCP8.5 scenario, the average global temperature is 0.7 to 3.7 degrees centigrade in the period from 1986- 2005, and the average global temperature in the period from 2018 to 2100 based on the RCP4.5 scenario is 0.5 to 1.8 degrees centigrade will increase.

2.6 Modeling efforts for the oil-sands region

Various methods have been used to predict the trend and sedimentation in rivers in different regions of the world. But because the present study is on the Athabasca River, several studies conducted in this area will be reviewed. Here we have a look at the experimental methods and numerical modeling done on the Athabasca River in the past years.

Garcia-Aragon et al. (2011) used an experimental method which was the rotating circular flume to define the characteristics of the Muskeg River sediments. In this study, experiments were performed on the simulation of sedimentation and flocculation behavior of these sediments. The results show that, if the Muskeg River bed-shear stress is around 0.265 Pa, any associated PAHs and 50% of the suspended material would be transported into the Athabasca River. Droppo et al. (2014) also used a 2-m annular flume to produce bed shear to assess sediment dynamics consistent

with 1, 3, and 7-day stabilization/biostabilization periods in Ells River. The results of this study showed that due to the high natural oil content, the sediments were very hydrophobic and the eroded sediments settled poorly. However, before these studies, Headley et al. (2001) used different environmental samples from selected branches in the oil sands area of the Athabasca River basin for gas chromatography/mass spectrometry (GC/MS) for polycyclic aromatic hydrocarbons (PAHs) and their alkylated analogs. to check their increase according to the tailings dam failure.

In recent years, due to the ease, lower cost, and higher accuracy of using numerical models, many studies have been conducted with this method. Khanna (2003) first used a 1D model called CDG1-D, which included rectangular sections to approximate the river section. Then Andrishak et al. (2008) studied the lower ice regime of the Athabasca River in the range downstream from Fort McMurray to Bitumount. In their study, they used a numerical ice process model, a one-dimensional river ice process model developed to investigate the potential effects of future outflow and climate change on the ice regime as well as the future water supply for the Athabasca River downstream of Fort McMurray. Pietroniro et al. (2011) also used a 1D model to simulate flow and transport processes in LAR.

One of the most important merits of one-dimensional models in comparison with two- and three-dimensional models is the simplicity of their governing equations, fewer computational nodes, and, as a result, lower calculation volume, shorter execution time, and easy analysis of their results. The conducted studies show that two-dimensional models are a good choice among one, two, and three-dimensional models, which, especially for long rivers, have less calculation time and volume and acceptable accuracy. Especially in the modeling of flows and sediments in LAR due to the complex morphology of rivers in cold climates with long periods of ice, it is very important to choose the appropriate model. Shakibaeinia et al. (2017) used the Mike-11 hydrodynamics, CST, and contaminant transport models. These models were strongly coupled with CRISSP-1D that are the 1D ice process model. The results of the simulation of hydrodynamic patterns, sediment transport, and the status and diversity of the selected metal components and PAH were correctly shown. So Dibike et al. (2017) investigated the influence of climate change on the sediment transport of the Athabasca river and its hydrodynamic regime. The simulations showed that changes in suspended sediment concentration are accompanied by a general increase in the average annual sediment in

the LAR and the Athabasca Peace Delta at the end of the century (2080), and the changes will be more than 50% compared to the period of 1980.

In general, due to the successful simulation of waste flow behavior patterns in this area, only a limited number of numerical modeling studies (1D and 2D) have been integrated to simulate the flow in LAR. Other studies conducted include the study of Dibike et al. (2018) mentioned and Hamjanin Mahdi et al. (2020). Dibike et al. (2018) investigated the consequences of tailings release on water quality and LAR sedimentation by simulating the destiny of sediments and chemicals considering a hypothetical failure using a 2D hydrodynamic model (EFDC). and Mahdi et al. (2020) also used a non-Newtonian numerical model (FLO-2D) to predict the overland flow of tailings and the potential leakage hydrograph to the LAR, in case of a tailings dam failure.

CHAPTER 3 APPROACH AND METHODOLOGY

So far, many studies have been conducted with the aim of numerical modeling the failure of tailings dams around the world. But choosing the most appropriate numerical model for simulation is still considered a challenge in this field. The non-Newtonian flow behavior of tailings flow that is created due to fine sediments and related chemicals requires us to provide solutions that can facilitate the numerical modeling of these types of flows. The method used in this study to answer these problems is as follows:

- The impact of tailings on the water body is unknown
- A limited number of studies had integrated numerical modeling (1D and 2D) to simulate flow in the LAR including Dibike et al. (2018) and Mahdi et al., (2020) but they assumed that the entire volume of the breach would flow into the LAR and did not consider the outflow and the tailings of overland flow from the breach to the river and they just used short-term scenarios.

Also, the global adjective determined for this study is a study of the impact of the tailings from the oil-sands tailings dam failure in the Lower Athabasca River and the context of climate change.

Generally, this study aims to improve the shortcomings of previous studies, for example:

- Settings up a hydrodynamic numerical model to model in Lower Athabasca River,
- Simulation of sediment and water quality based on spill hydrographs from the work of Mahdi et al. (2020), considering various flow scenarios, and
- Its historical conditions and future conditions.

This study is divided into two parts and in both parts of this study two-dimensional numerical modeling system of Environmental Fluid Dynamics Code (EFDC) was used. The sediment transport module in the EFDC model solves the sediment transport equation for cohesive and non-cohesive sediments in different sizes of sediment particles. In the first part, the mentioned model was used to simulate the flow due to a break in one of the big tar tailing dams. In an initial attempt to quantify the such environmental impact, we set up, validate, and applied EFDC 2D numerical model for the Lower Athabasca River and investigated the impact of different spill scenarios on

the water and sediment quality of the river (see Dibike et al. 2018). This study however used a simple analytical method to calculate the spill hydrograph. Later was used another model to accurately predict the flow of tailing material and their spill to the Athabasca (see Mahdi et al. 2019). In this, it only studied what happens before the spill and did not consider the fate of tailing materials in the river.

In the second part, this simulation is done separately to predict future years. This simulation is also done separately to predict future years. Model simulations and related boundary conditions are performed for the period from September 1 to September 30, 2045, to investigate the impact of future climate change. Details and results are shown in Chapter 04.

3.1 Simulation-based on historical data

Numerical model simulation and the effects of hypothetical tailings release from the selected MLSB pond (Mildred Lake Settling Basin) on sediments, its transport and chemical deposition of LAR, and the effects of oil rock tailings release in the historical information section is investigated in 5 scenarios, which include: a scenario based on an average flow condition, the spills with 25-year and 50-year floods and a flood wave with the return periods of 25-year and 50-year a few days after the spill event.

3.2 Simulation-based on future data

Numerical model simulation and the effects of hypothetical tailings release from the selected MLSB pond in the future information section is investigated in 5 scenarios, which include: a scenario based on an average flow condition, the spills with 25-year and 50-year floods, and a flood wave with the return periods of 25-year and 50-year a few days after the spill event.

The methodology of this study is summarized in the following diagram (Figure 3.1).

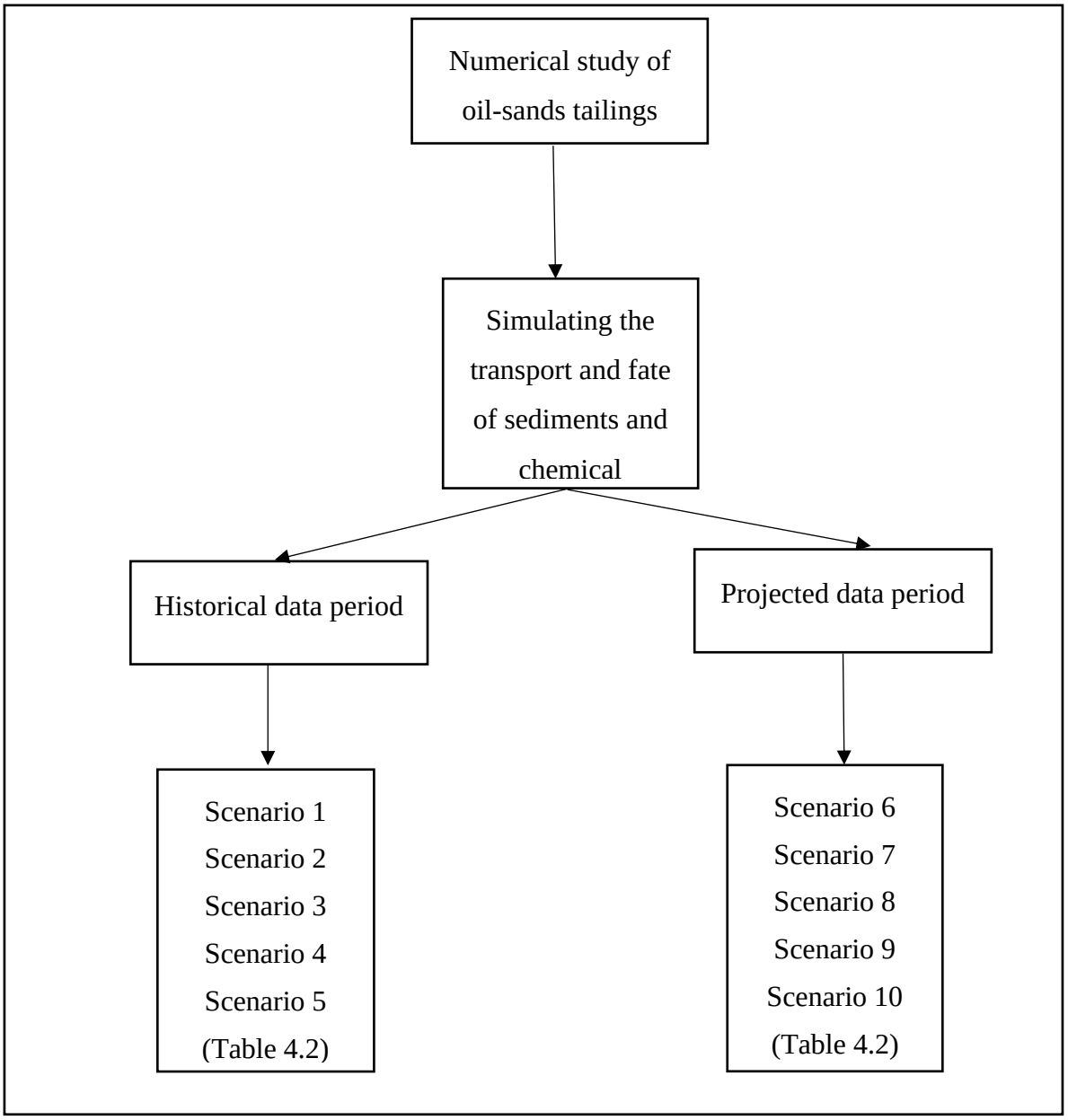

Figure 3.1 Explanatory diagram of the methodology followed in this study

CHAPTER 4 METHODS AND RESULTS

This chapter investigates the transport and fate of Oil Sands tailings, discharged to the LAR, in an event of a tailing dam break (figure 4.1), using a two-dimensional hydrodynamic and sediment transport numerical model. The simulations are done considering different river flow scenarios. Various historical and future flood scenarios (due to climate change) are considered and their impact on the fate and transport of spilled pollutants is investigated. A tailings storage facility in the lower Athabasca Oil Sands region is selected as the case study. The lower Athabasca Oil Sands region is selected as the case study. This choice was made due to the proximity of this tailings dam to the lower Athabasca River, its high capacity, and its high impact on the region. Then the effects of hypothetical tailings release scenarios due to sudden breaches on it are investigated. In this study, simulations of the hydrodynamic model and sediment transport for future periods to determine suspended sediment concentrations (SSC) and sediment in LAR are discussed.

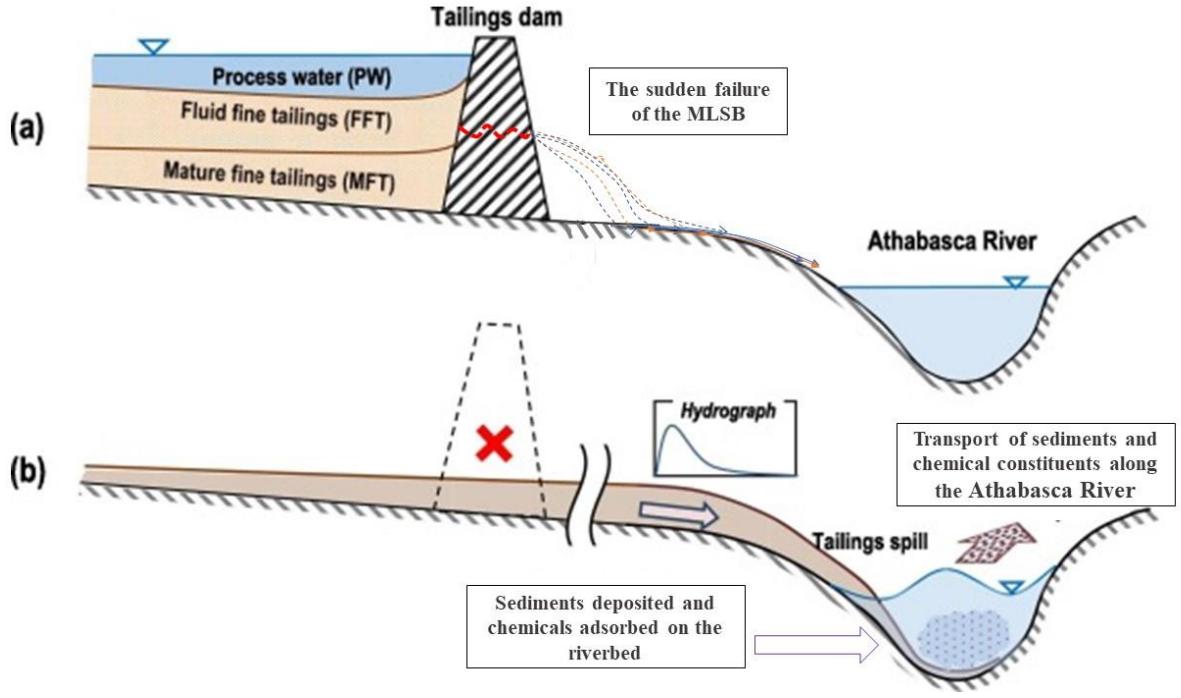

Figure 4.1 schematic of (a) typical oil-sands TSF Oil Sands tailings and their constituents in the sudden failure, (b) post-breach transport processes

4.1 Study area and data

4.1.1 Study area

The study area is a ~200 km reach of Lower Athabasca River (LAR) in northern Alberta in Canada, which begins at the confluence of the Athabasca and Clearwater rivers near the town of Fort McMurray (in Alberta, Canada) and extends for around 32 km downstream of the Firebag River (around Oldfort) (Figure 4.2). Major tributaries within the study are the Ells River, Steep-Bank River, Muskeg River, Firebag River, and MacKay River. The study reach is meandering and braided with vegetated islands and cuts through bitumen deposits. It is also adjacent to the oilsands mining developments, and several TSFs. Here the tailing spill is based on the hypothetical tailing dam break in an example TSF, i.e., the Mildred Lake Settling Basin (MLSB) or Syncrude Tailings Dam. The MLSB is an embankment dam located around 40 km north of Fort McMurray, at the northern end of Lake Mildred. This tailings dam has a storage capacity of 350 × 106 cubic meters. The total volume, fluid fine tailings (FFT) volume, and process water volume of 540, 120, and 12 million cubic meters, respectively (Mahdi et al. 2020).

4.1.2 Hydrometric and climate data

Historical hydrometric data (flow rate and water level) and sediment data, which were used for boundary conditions and validation of the model, were obtained from the Water Survey of Canada (WSC), for various stations along the mainstream and in major tributaries (near confluences).

The future flow data (under changing climate) are provided by Dibike et al., (2018) and are based on the outcome of the VIC hydrologic model for various climatic scenarios. The scenarios used in this study are based on the latest General Circulation Model, GCM, a projection by the year 2100 (the time frame used is 2038-2100), made under the CMIP5 framework and the French CNRM (Voldoire et al., 2013) model for two emission scenarios (RCP4.5 and RCP8.5). Finally, the scenarios of this study include CanESM SD45, CanESm SD85, and CNRM SD45. Table 4.1 provides example flow discharge statistics for the upstream (inflow) boundary. More detailed information can be found in Dibike et al., (2018). The future water level and sediment data for the future period are estimated according to the assumption that the historical rating curves will be valid for the future period.

Table 4.1 flow data statistic for the upstream boundary, based on the historical and projected (under changing climate) data

Data period		Upstream discharge (m^3/s)		
		Average	**25-years return period**	**50-years return period**
Historical (1956-2011)		582	4418	4933
Projected	**CanEsm SD45**	786	3678	4067
	CanEsm SD85	845	3663	4006
	CNRM SD45	733	3510	3915

4.2 Numerical model

Here we use EFDC two-dimensional (2D) hydrodynamic, water quality, sediment transport modeling system with EFDC Explorer pre- and post-processor software, developed by DSI Consulting Group (Craig, 2013). It has been applied and validated in several past studies on modeling the fate and transport of sediment and chemicals in LAR (e.g., in Dibike et. al 2018, Kashyap et al., 2017). For the hydrodynamics, it solves the 2D depth-averaged Reynolds-averaged Navier–Stokes equations using a second-order finite difference scheme on a staggered grid. It also solves advection-diffusion equations for the transport of non-cohesive and cohesive sediments. The model can deal with the transport of chemical compounds dissolved in water and adsorb to the sediments in the water column and bed (Kashyap et al. 2017). Here we used a 2D cartesian grid, with a uniform resolution of 75 m (~46,000 total cells), to represent LAR computational domain. For the inlet (upstream and tributaries) boundary condition the flow discharge and concentrations (or concentration-discharge rating curves), and for the outlet the water level and zero gradient concentration were used. This EFDC has been calibrated and validated for LAR as explained in Kashyap et al. (2017) and Dibike et al. (2018).

In this study, a 30-day simulation period with various flow scenarios (under the current and projected flow conditions) including tailings spill from the hypothetical breach of the selected TSF is considered.

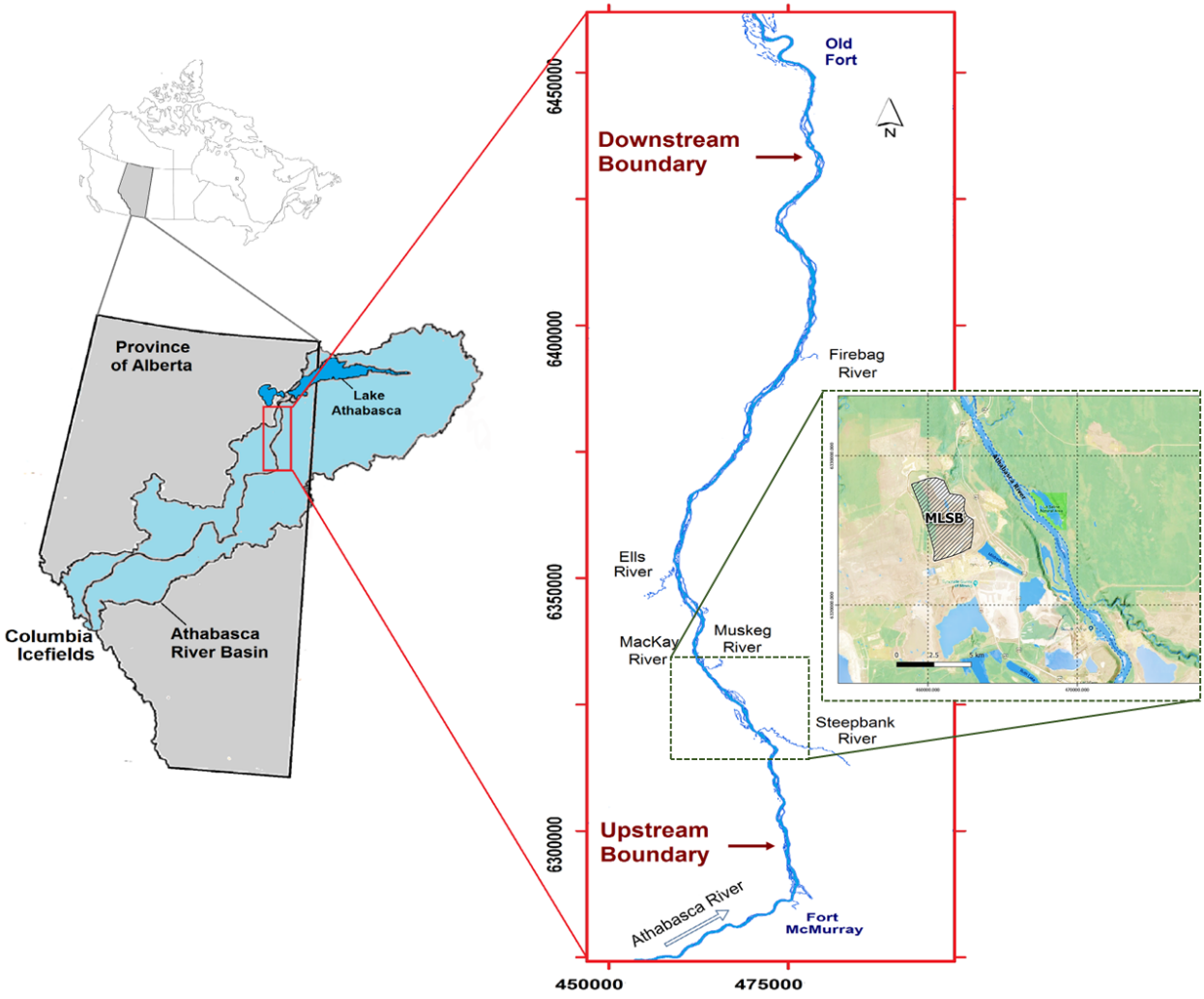

Figure 4.2 locations of the Mildred Lake Settling Basin (MLSB) and oil-sands tailings storage facilities around the Lower Athabasca River (LAR) (based on Mahdi et al, 2018)

4.3 Breach hydrograph

Following the hypothetical breach of a TSF, the tailing slurries flow overland through the drainage course and spill into the river. For the case of MLSB hypothetical breach, the simulations of Mahdi et al (2020) using a non-Newtonian dam-break and overland flow model, showed two major spill locations (points 1 and 2 in Figure 4.3). The resulting spill hydrograph (Figure 4.3 (b)) shows that point 1 is the main point of spill into the LAR. These spill flow hydrographs are used here as a lateral inflow boundary condition to the LAR. The spill sediment and chemical concentration are based on estimations from Dibike et al (2018).

(a)

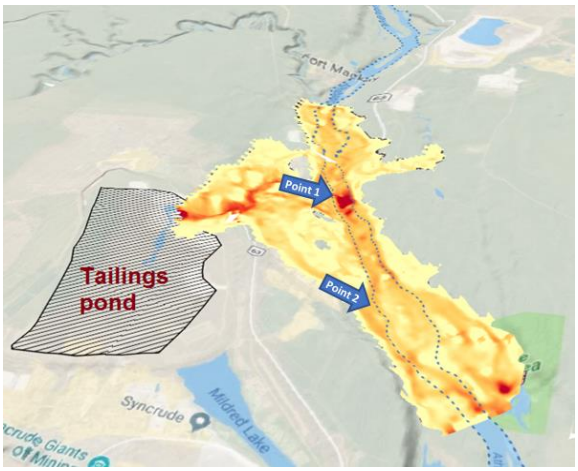

(b)

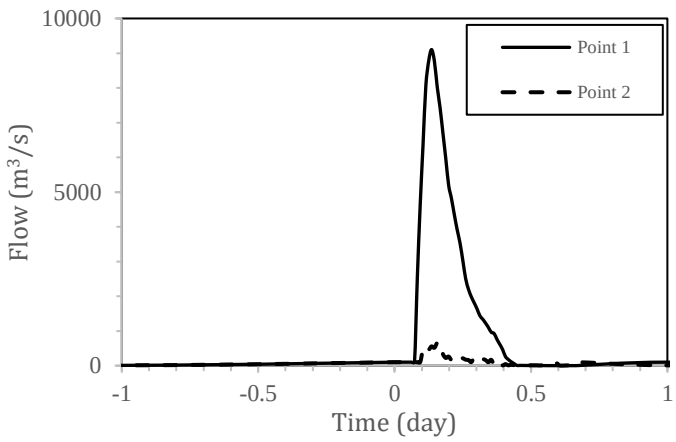

Figure 4.3 MLSB hypothetical tailings dam breach runout, overland flow, and spill to the LAR through two points, based on the simulations of Mahdi et a; (2020), (a) flow extent, (b) spill hydrographs

4.3.1 Tailings pond breach scenarios

A study by Dibike et al (2018), which considered a spill in average river flow conditions, underscored the fact that a part of the spilled sediments and associated chemicals may deposit within the bed, with the potential of resuspension in future floods. Therefore, here we have considered various flooding scenarios to better quantify the short-term and long-term consequences of a potential tailing dam breach. Table 4.2 summarizes the study scenarios. This includes ten scenarios with various floods during and after a tailing breach, based on the historical river flow data as well future flows, under changing climate (based on the project flows from 1957 to 2019). Table 4.1 summarizes the amount of flow information in each scenario at the upstream entrance of the study area.

Table 4.2 simulation scenarios based on existing historical data and future data

Scenarios	Description
Based on the historical data	
SN1	Spill happens in an average flow condition
SN2	Spill happens with a 25-years flood
SN3	Spill happens with a 50-years flood
SN4	A flood wave with a return period of 25 years happens a few days after the spill event
SN5	A flood wave with a return period of 50 years happens a few days after the spill event
Based on the future projected data	
SN6	Spill happens in an average future flow condition
SN7	Spill happens with a 25-years flood
SN8	Spill happens with a 50-years flood
SN9	A flood wave with a return period of 25 years in the future data happens after a few days we have a spill
SN10	A flood wave with a return period of 50 years in future data happens after a few days we have a spill

4.4 Results and discussion

The results of hydrodynamic model simulation and the effects of the release of hypothetical tailings from the selected pond MLSB (Mildred Lake Settling Basin) on sediments, its transporting and chemical deposition of LAR in two parts, and the effects of the release of oil-sands tailings on historical and future data are presented below.

4.4.1 Impact on the hydrodynamic

Figure 4.4 shows the flow depth variation within the LAR following the spill event based on scenario SN1. The spill of tailings at designated points of the river causes an immediate increase in river water level at the spill location that later propagates downstream and upstream. Figure 4.4 also shows the amount of discharge for thirty days from the time the tailings flow spills for SN1 that is caused to increase in the discharge and water level along the river. In this diagram, the reference time (T = 0) for all results corresponds to the moment of the tailings breach and spill. Results are particularly provided downstream of the spill point (DS spill location, *X*=463300 m E, *Y*= 6332280 m N), downstream of the Firebag (DS Firebag, X= 478180 m E, Y= 6401380 m N), downstream of the study area (DS study area: *X*=477751 m E, Y: 6436461 m N), and the spill point. The peak of the incoming flow to the LAR occurs immediately after the spill and reaches up to 9000 (m^3/s) which is about 25 times the average flow and the peak reaches the downstream in about 36 hours (Figure 4.5).

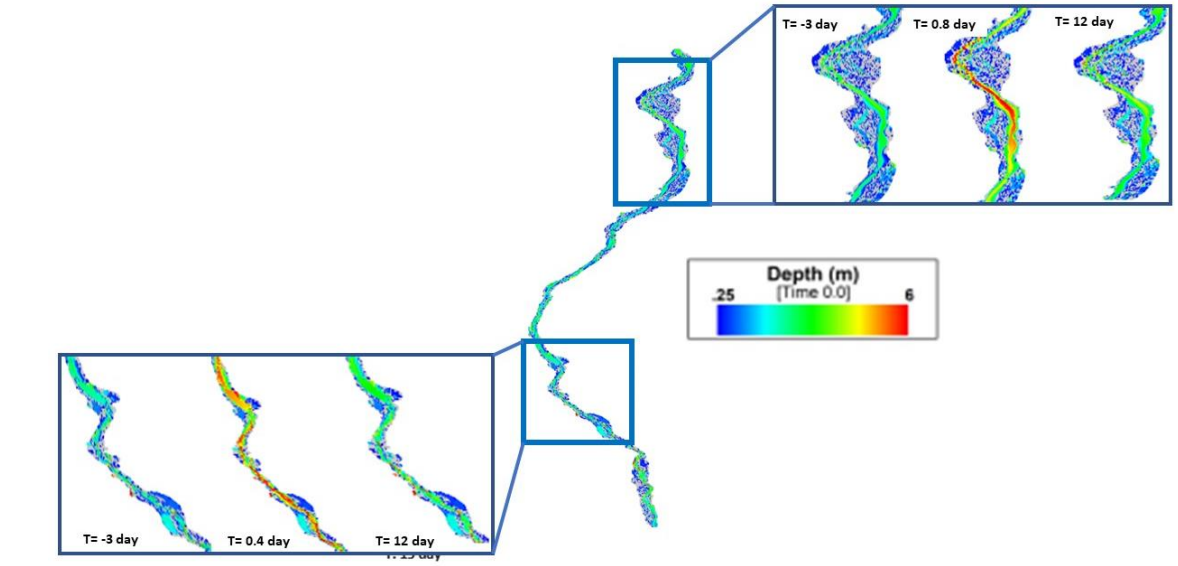

(b)

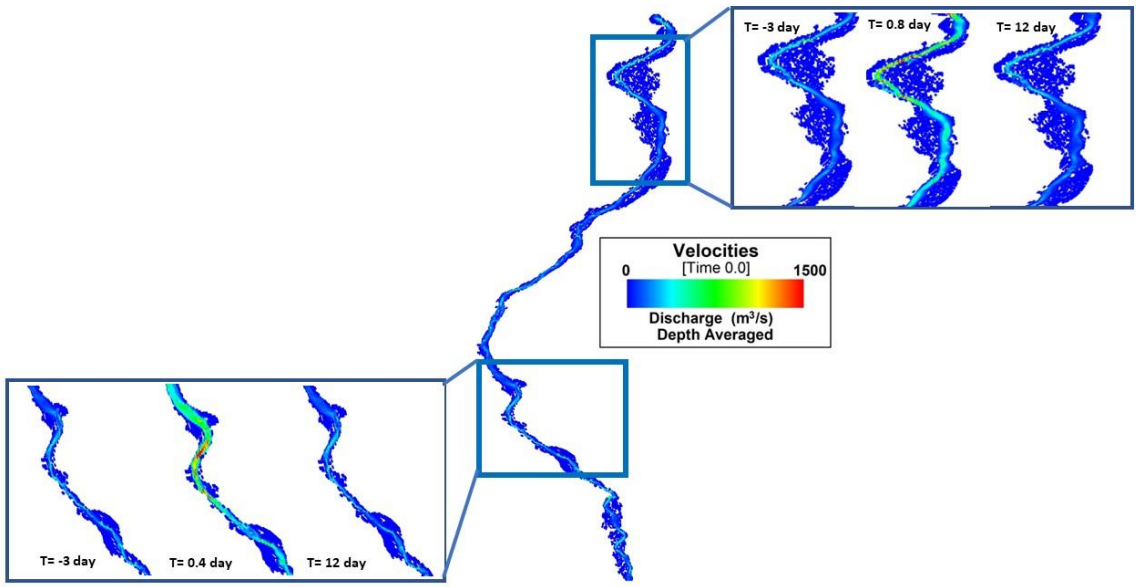

Figure 4.4 simulated water depth progress and discharge at two different locations from MLSB hypothetical tailings spill in SN1

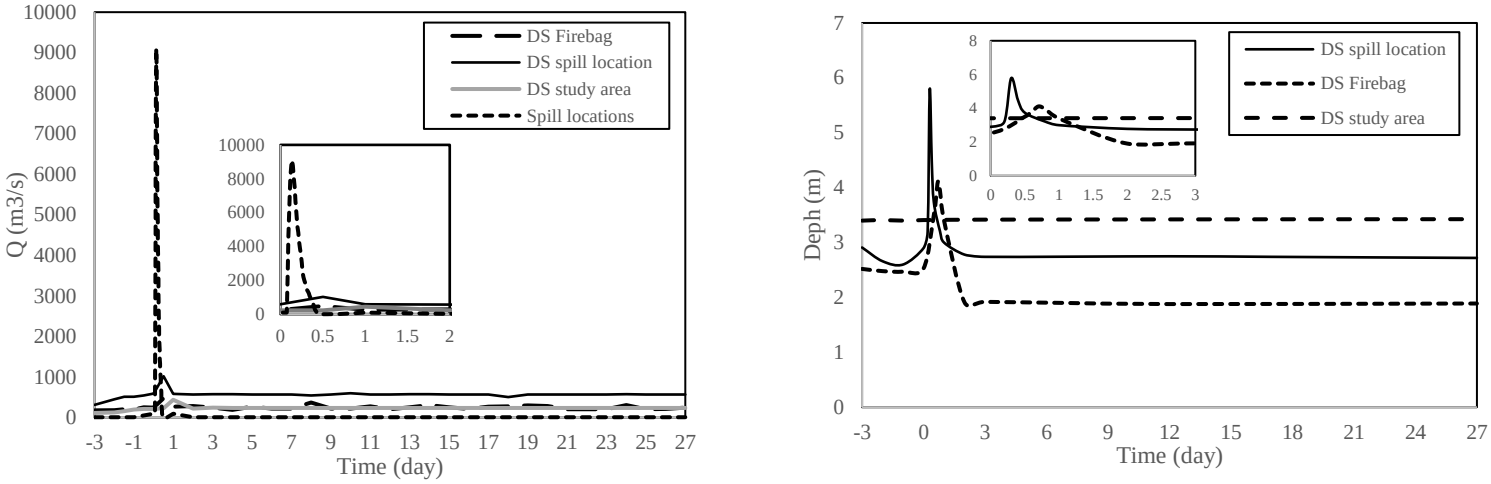

Figure 4.5 simulated flow discharge and water depth for various locations along LAR, based on scenario SN1

The longitudinal profile plots in Figure 4.6 show that the mass/concentration in the riverbed generally increases downstream of the spill points and becomes almost constant upon reaching a maximum. Of course, we should not ignore the influence of the derivation streams from the branches connected to the LAR. After a few days from the time of the spill, the amount of sediment mass deposited in the riverbed in the downstream direction increases more than in the first days, and this is due to the washing of the bed sediments in the upstream and its transfer to the downstream and erosion during high flow that increases over time. This indicates that the sediments and chemical compounds deposited in the riverbed will settle in the riverbed for a long time after the sediments and chemical substances dissolved and suspended in the water column are removed. Therefore, it increases the possibility of transmission due to heavy floods to the Peace Athabasca Delta (PAD) in the future.

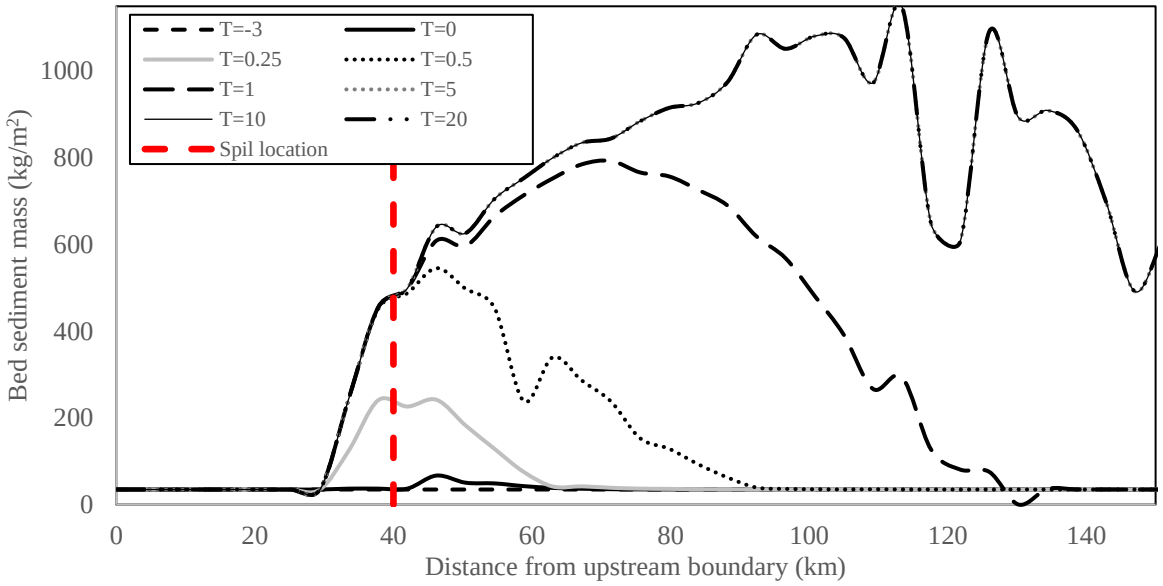

Figure 4.6 the simulation of the longitudinal profile for sediment concentration mass in the LAR riverbed after the hypothetical dam-breach

A sudden increase in the concentration of suspended sediment in the water column is observed in all scenarios immediately after the spill at the spill site. The water column concentration reaches its initial value after around 90 minutes, as the sediments are transported downstream (Figure 4.7). Of course, sediment transfer will not be complete because part of the sediment will settle in the riverbed. The amount of lead in the water column also shows a similar approach to the sediments. Peak values of the chemical concentration are observed at the same time as the failure event, i.e. T=0, and Figure 4.7 shows that their magnitude decreases by about 50-60% downstream, depending on the scenarios. This amount of difference downstream and spill points from the tailings dam can greatly affect the uptake of sediments and related chemicals released into the riverbed. There is a fact that with the release and release of tailings along the river, a percentage of suspended sediments and chemicals are deposited in the riverbed. It is also important to state that in this study, 6 chemicals were investigated, including lead, vanadium, arsenic, pyrene, phenanthrene, and benz[a]anthracene chrysene (BAC). Due to the high volume of simulation and the similarity of the trend of these chemicals, lead was chosen as the chemical that can show their trend well.

According to the three climate model scenarios (CanESM SD45, CanESM SD85, and CNRM SD45), the simulation was repeated based on each future scenario to provide a range of uncertainty in the result. In all scenarios, the maximum sediment concentration in the water column occurs at approximately the same time, and almost all three climate model scenarios show a general trend (see the appendix for details). Therefore, in the following study, Due to the slight difference between the results of climate model scenarios the Canadian model with the high emission scenario of CanESM SD85 will try to be used for data analysis. In Figure 4.7, Scenario 6 shows that the precipitate increase in the sediment concentration in the vicinity of the spill site starts from the T=0 day and reaches the release concentrations of about 380 g /l. Then, 24 hours later, they reach downstream of the study area and after about 70 hours from the start, it comes out completely from downstream. It can also be seen from the release points downstream that the concentration of the water column gradually decreases, this is because part of the sediments settles in the riverbed. It should also be noted that the spill happened on T=0 day. Still, the peak occurs on day T= 0.2 or 0.3 because the effect of backwater effect together with advection/dispersion mechanisms causes these concentrations to be transported upstream for several kilometers and re-flow downstream (Dibike et al., 2018).

In general, Figure 4.7 shows that in all the scenarios, the behavior of tailings along the river follows a similar process and they travel along the river at the same time and reach downstream. Also, in all scenarios, this phenomenon is evident that a significant amount of sediments and lead are deposited in the river bed. For scenarios with average data (i.e. scenarios 1 and 6), this amount of sedimentation material is about 40%, which shows a lower percentage of material sedimentation in the river bed after the failure of the tailings dam, compared to other scenarios. However, in other scenarios, up to 60% sedimentation and lead absorption by the riverbed occur.

(SN1)

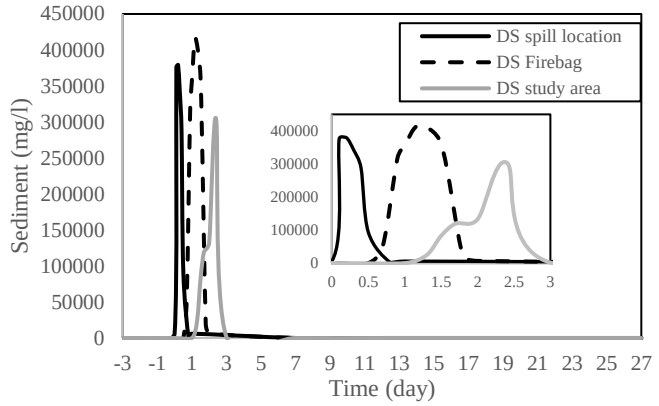

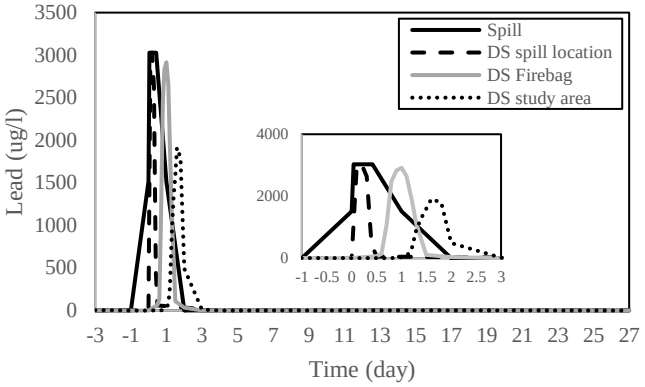

(SN2)

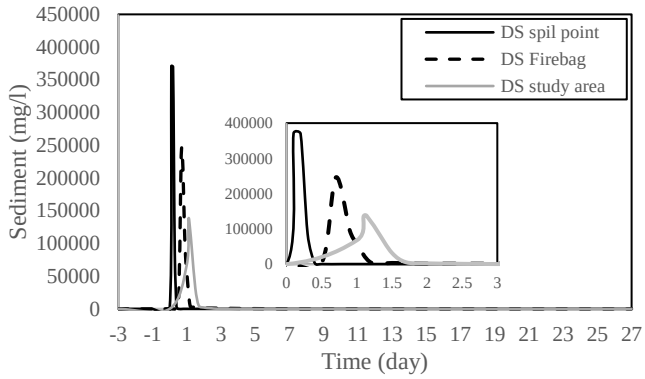

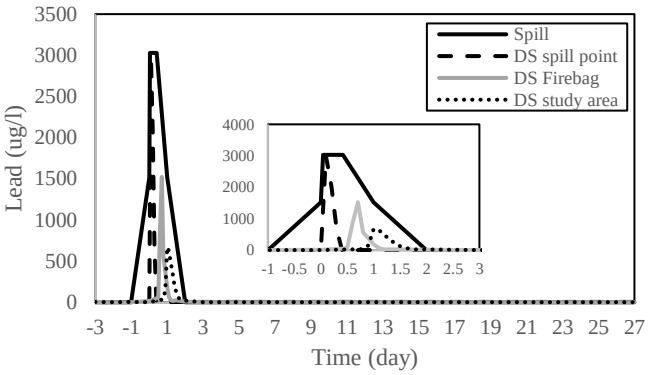

(SN3)

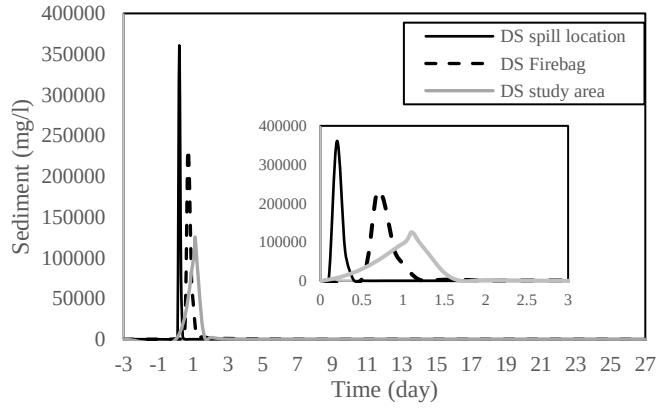

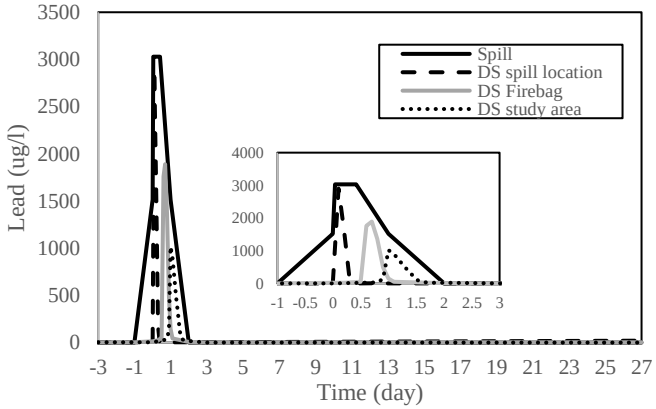

Figure 4.7 the simulated time series of sediment and Lead in the depth-averaged water column at different locations along with the LAR respective to a hypothetical tailings pond breach for 10 scenarios (continuous)

(SN4)

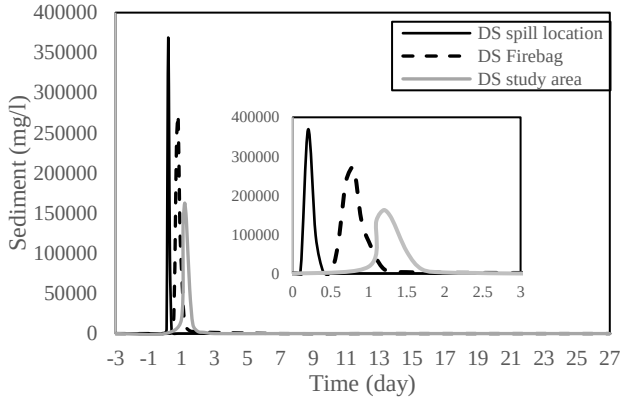

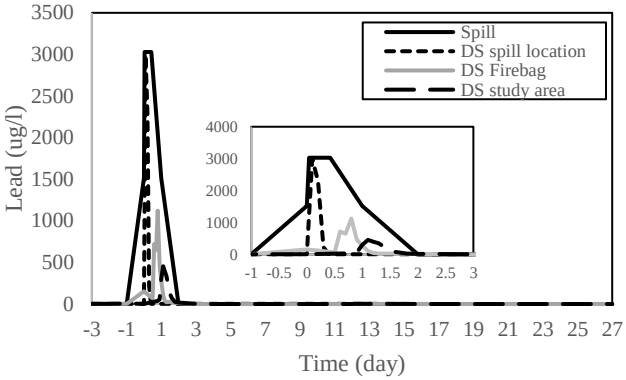

(SN5)

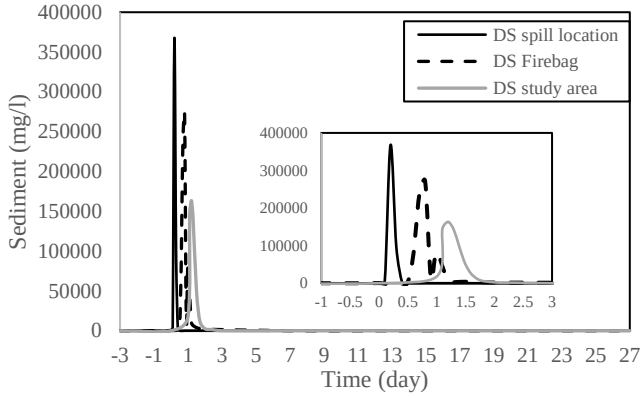

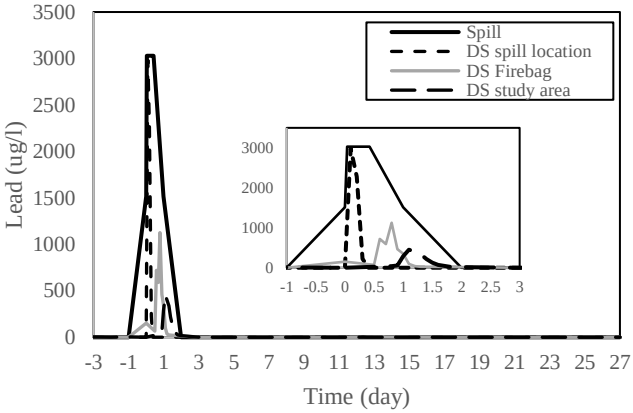

(SN6)

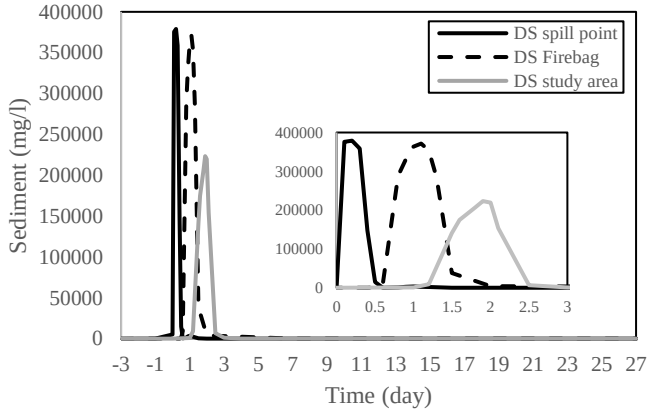

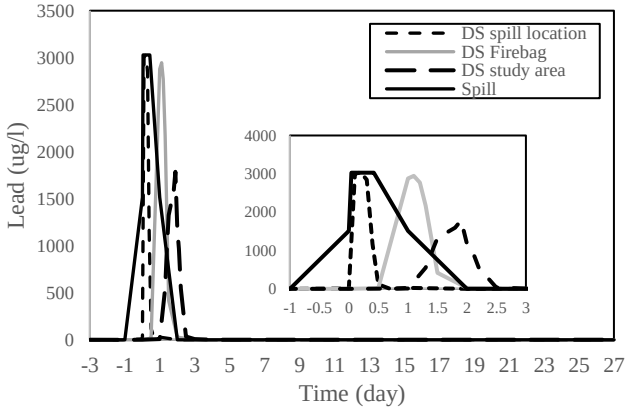

Figure 4.7 the simulated time series of sediment and Lead, in the depth-averaged water column at different locations along with the LAR respective to a hypothetical tailings pond breach for 10 scenarios (continuous)

(SN7)

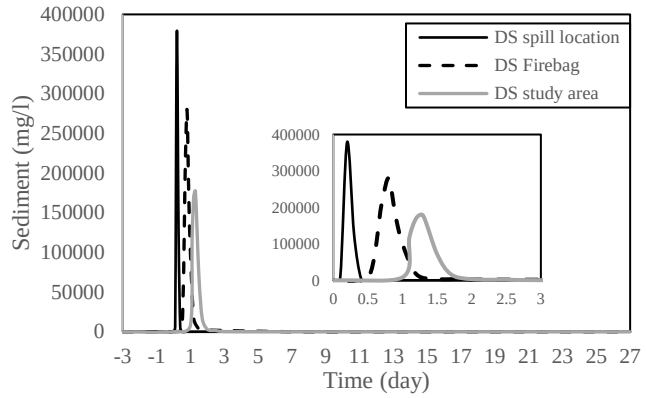

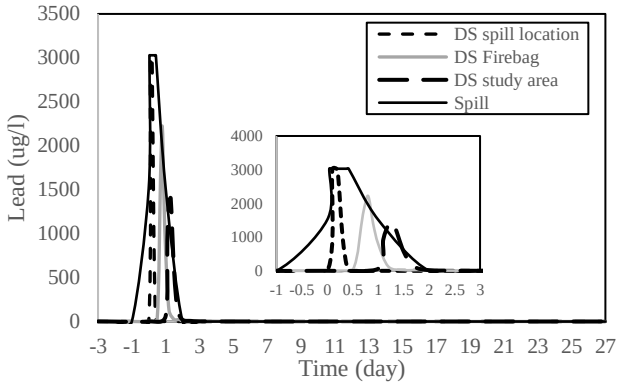

(SN8)

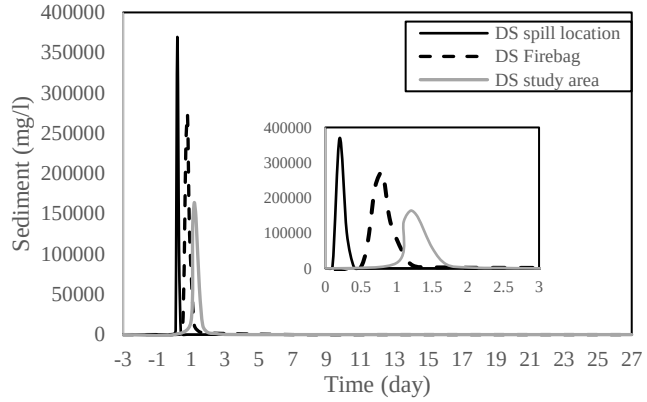

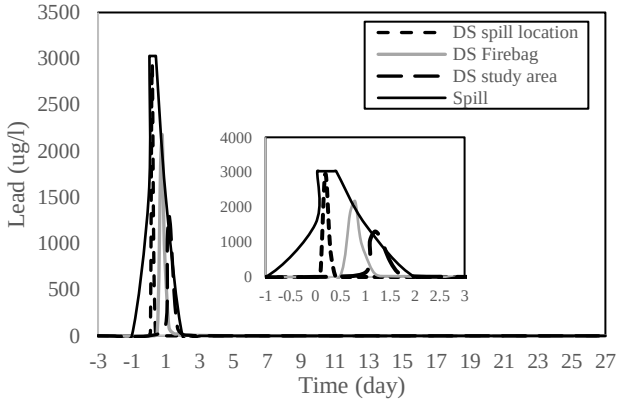

(SN9)

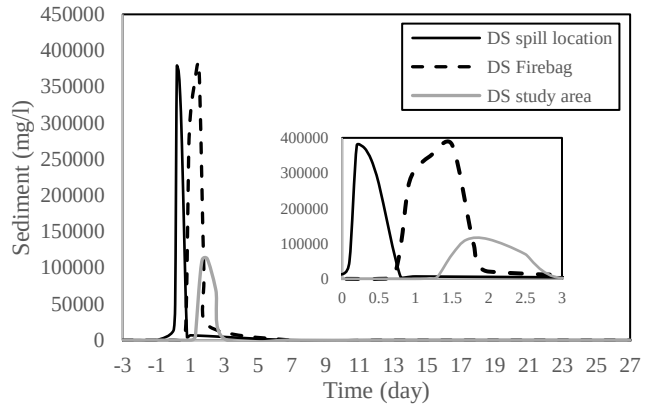

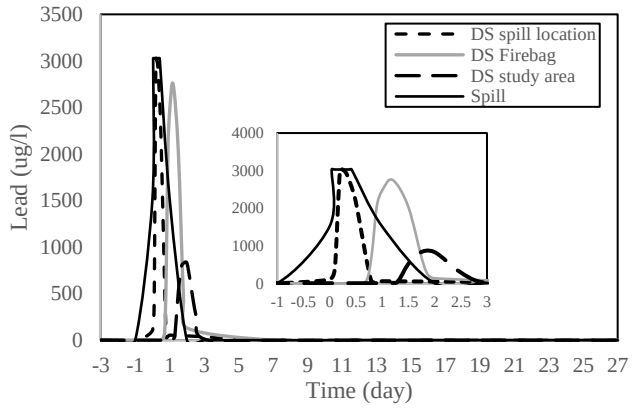

Figure 4.7 the simulated time series of sediment and Lead, in the depth-averaged water column at different locations along with the LAR respective to a hypothetical tailings pond breach for 10 scenarios (continuous)

(SN10)

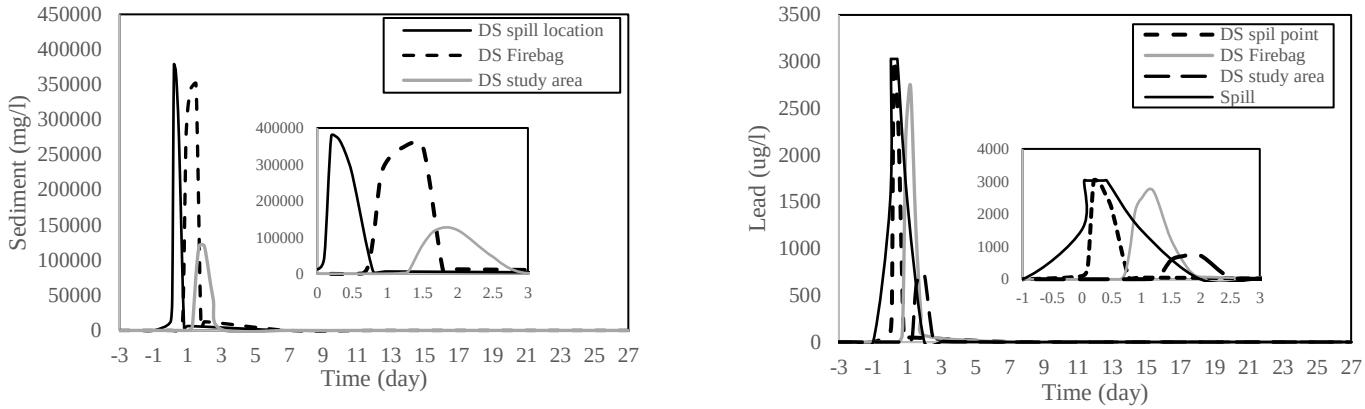

Figure 4.7 the simulated time series of sediment and Lead, in the depth-averaged water column at different locations along with the LAR respective to a hypothetical tailings pond breach for 10 scenarios

The amount of upstream inflow (Table 4.2) for future scenarios except scenario 6 is lower than the value of upstream inflow for historical data scenarios. Therefore, Figure 4.8 shows the higher concentration value in future scenarios. For example, if scenario 2 is compared with scenario 7, the concentration of toxic substances in the water column for scenario 7 downstream of the study area (DS Study area) is about 500 ug/l more than scenario 2 at peak flow. Similarly, these differences between the scenarios are tangible in Figure 4.8.

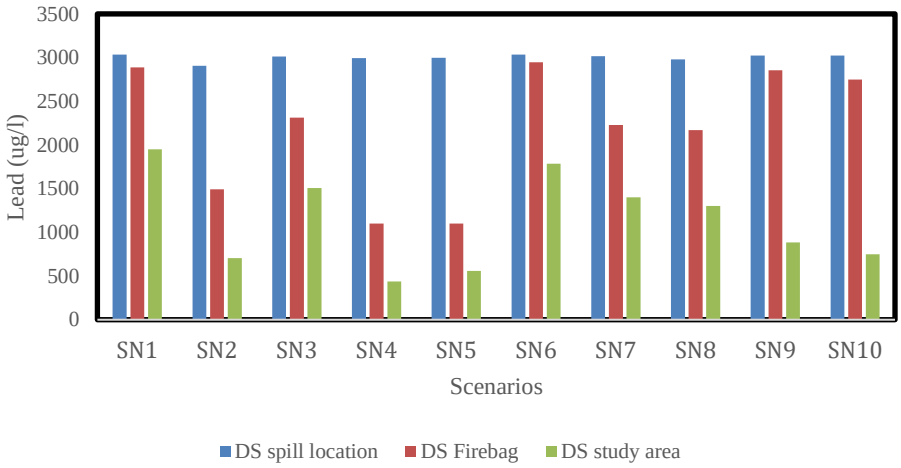

Figure 4.8 the peak of lead and sediment concentration in the depth-averaged water column at DS spill point, DS Firebag, and DS study area after a hypothetical tailings release on 10 scenarios

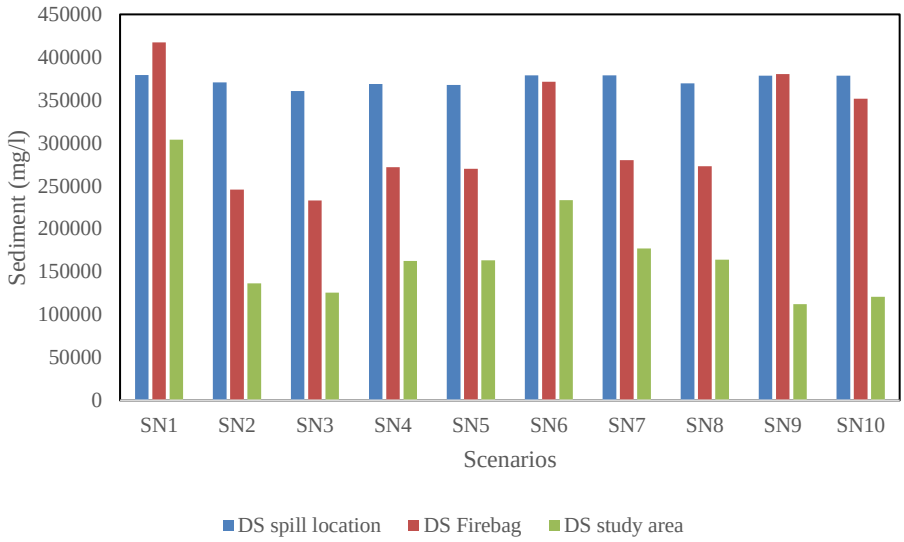

Figure 4.8 the peak of lead and sediment concentration in the depth-averaged water column at DS spill point, DS Firebag, and DS study area after a hypothetical tailings release in 10 scenarios

Part of the suspended sediments and chemicals settle in the riverbed along with the LAR and this is quite evident in figure 4.6. Because with the release of tailings in the LAR, suspended sediments and chemicals begin to spread downstream, and when they reach the downstream of the Firebag, the concentrations decrease by 50%. Also, especially in scenarios 4 and 5, this amount of concentration decreases to 60% downstream of the study boundary, which can be one of the reasons for their settlement in the riverbed. Therefore, in Figure 4.9, a view of the simulated results is considered for suspended solid and also Lead in the water column after a flood (on the 12th day of the hypothetical dam breach). Figure 4.9 shows what will happen if a flood occurs after the dam breaks. It shows the value of suspended solids from the 12th day that the hypothetical flood occurred, which shows higher amounts in the water column compared to the chemical concentration leached from the riverbed. This hypothetical flood started 24 hours from upstream of the study area and then came out from downstream.

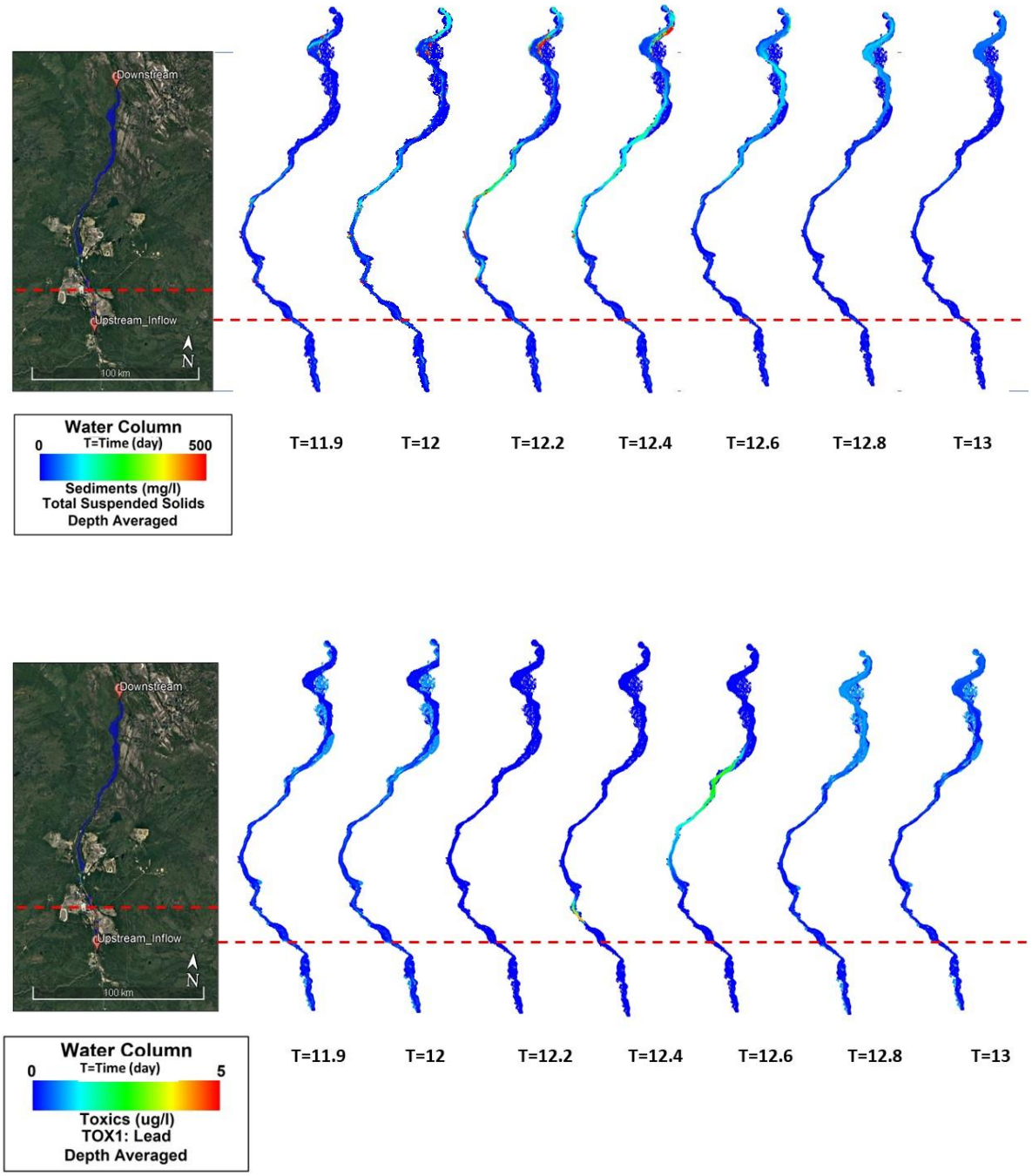

Figure 4.9 the time sequence of simulated Total Suspended Solids (TSS) and the amount of one toxic (lead) in the depth-averaged water column after a flood on the 12th day based on scenario 4.

CHAPTER 5 CONCLUSION AND RECOMMANDATIONS

The two-dimensional EFDC numerical model was used to simulate the hypothetical failure of a tailings dam to estimate flood and flow changes according to ten scenarios. The Low Athabasca area in Alberta was considered the study area. Two spill hydrographs were applied in this study. These spill flow hydrographs were applied as lateral flow boundary conditions to the LAR. The model was then used to simulate the MLSB dam failure, which was considered near a drainage system connected to the lower Athabasca River. The simulations of the model showed the ability of the model to model flows by estimating flood area, water depth changes, and downstream flow.

This hydrodynamic model was used to simulate the deposition of sediment and transport as well as the transport and absorption of selected lead toxic substances in LAR. The simulation showed that about half or more of the sediments and chemical compounds entering into the LAR almost completely leave after 24 hours of the spill happen, while the rest is deposited in the river. Almost for all scenarios, about 50% of the sediment mass and 30% of the lead mass are moved out from the study area, and the rest remain in it, and most of these depositions are in the parts close to the spill locations. The sediments/chemicals that are deposited in the river bed showed their effect on the ecosystem and water quality of the river in the long term, and with the occurrence of a flood 12 days after the dam failure and the tailings entered the river, it increased the suspended sediments and existing chemicals along the river.

In this study, the possible effect of climate change on the sediment transport of LAR and the hydrodynamic regime is also investigated and these changes are more significant under changing climate. Climate predictions were made using the VIC hydrological model outputs related to CNRM and CanEMS under both of the two emission scenarios RCP8.5 and RCP4.5. The simulation results of the scenarios present an entire increase in flow for all future scenarios. In general, these climate changes (increased precipitation and temperature) in the Athabasca watershed are anticipated to affect the hydrological regime in the LAR system. In general, the hydrodynamic simulation performed in LAR shows an increase in flow speed and water level in the future, which will lead to an overall increase in flow and sediment transport in LAR.

In general, a limited number of numerical models are capable of simulating tailings streams due to their complex non-Newtonian behavior. The EFDC numerical model is one of the models that has been able to demonstrate its ability to simulate the non-Newtonian behavior of tailings materials

resulting from the failure of tailings dams. This study proceeded with the assumption that the tailings failure hydrograph remains unchanged as it enters the LAR as a point source, which any deficiency in these assumptions may underlie any changes in the concentrations of sediments and chemicals introduced. This model has been one of the most widely used models to simulate the behavior of tailings materials in the lower Athabasca River in these years. Therefore, it is suggested that more research be done to compare this numerical model with other complex models for simulating in this area. This model can also be used in other regions with different climates.

ACKNOWLEDGEMENTS

I would like to thank Yonas Dibike for his guidance and for kindly and compassionately guiding me in this way.

REFERENCES

Akre, C. J., Headley, J. V., Conly, F. M., Peru, K. M., & Dickson, L. C. (2004). Spatial patterns of natural polycyclic aromatic hydrocarbons in sediment in the lower Athabasca River. Journal of Environmental Science and Health, Part A, 39(5), 1163-1176.

Allen, E. W. (2008). Process water treatment in Canada's oil sands industry: I. Target pollutants and treatment objectives. Journal of Environmental Engineering and Science, 7(2), 123-138.

Andrishak, R., Abarca, J., Wojtowicz, A., & Hicks, F. (2008). Freeze-up study on the lower Athabasca River (Alberta, Canada). Paper presented at the Proceedings of the 19. IAHR international symposium on ice: using new technology to understand water-ice interaction.

Arora, V. K., Scinocca, J., Boer, G., Christian, J., Denman, K., Flato, G. & Merryfield, W. (2011). Carbon emission limits are required to satisfy future representative concentration pathways of greenhouse gases. Geophysical Research Letters, 38(5).

Ashworth, P. J., Best, J. L., Roden, J., Bristow, C. and Klaassen, G. 2000. Morphological Evolution and Dynamics of a Large, Sand Braid-Bar, Jamuna River, Bangladesh. Sedimentology. (47): 533-555.

Baird, D., Banic, C., Bickerton, G., Burn, D., Dillon, P., Droppo, I. & Kelly, E. (2011). Lower Athabasca Water Quality Monitoring Program. PHASE 1□ Athabasca River Mainstem and Major Tributaries. Energy Resources Conservation Board: Ottawa, Ontario, Canada, 90.

Burgar, J., Sztaba, A., & Region, L. A. (2015). Aerial Ungulate Survey (2015), Moose in WMU 519. Environment and Parks, Government of Alberta, Lower Athabasca Region, Fort McMurray.

Canadian Association of Petroleum Producers (CAPP). Website: www.capp.ca www.oilsandstoday.ca.

Chaudhry, M.H. and Flow, O.C., 1993. Prentice-Hall. Englewood Cliffs, New Jersey, 7632.

Clemente, J.S. & Fedorak, P.M., 2005. A review of the occurrence, analyses, toxicity, and biodegradation of naphthenic acids. Chemosphere, 60(5), pp.585-600.

Conly, F., Crosley, R., & Headley, J. (2002). Characterizing sediment sources and natural hydrocarbon inputs in the lower Athabasca River, Canada. Journal of Environmental Engineering and Science, 1(3), 187-199.

Cunge, J., 1980. Practical aspects of computational river hydraulics. Pitman Publishing Ltd. London,(17 CUN), 1980, 420.

Dalrymple, R. A. 1985. Introduction to Physical Models in Coastal Engineering, in Physical Modeling in Coastal Engineering. Rotterdam, Netherlands, pp 3-9.

Dennis, I. A., Macklin, M. G., Coulthard, T. J. & Brewer, P. A. (2003). The impact of the October–November 2000 floods on contaminant metal dispersal in the River Swale catchment, North Yorkshire, UK. Hydrological Processes, 17(8), 1641-1657.

Dibike, Y., Prowse, T., Bonsal, B. & O'Neil, H. (2017). Implications of future climate on water availability in the western Canadian river basins. International Journal of Climatology, 37(7), 3247-3263.

Dibike, Y. B., Shakibaeinia, A., Droppo, I. G. & Caron, E. (2018). Modelling the potential effects of Oil-Sands tailings pond breach on the water and sediment quality of the Lower Athabasca River. Science of the Total Environment, 642, 1263-1281.

Droppo, I. G., D'Andrea, L., Krishnappan, B. G., Jaskot, C., Trapp, B., Basuvaraj, M. & Liss, S. N. (2015). Fine-sediment dynamics: towards an improved understanding of sediment erosion and transport. Journal of Soils and Sediments, 15(2), 467-479.

Edmonds, W.A., 2020. EFDC+ DOMAIN DECOMPOSITION: MPI-BASED IMPLEMENTATION.

Environment Canada, 2011. Lower Athabasca Water Quality Monitoring Program, Phase 1, Athabasca River Mainstem and Major Tributaries. Minister of the Environment, Gatineau, QC.

Eum, H.-I., Dibike, Y. & Prowse, T. (2017). Climate-induced alteration of hydrologic indicators in the Athabasca River Basin, Alberta, Canada. Journal of hydrology, 544, 327-342.

Formann, E., Habersack, H.M., Schober, S.T. 2007. Morphodynamic river processes and techniques for assessment of channel evolution in Alpine gravel bed rivers. Geomorphology, 90, 340-355.

Fourie, A., Blight, G. & Papageorgiou, G. (2001). Static liquefaction as a possible explanation for the Merriespruit tailings dam failure. Canadian Geotechnical Journal, 38(4), 707-719.

Frank, R.A., Roy, J.W., Bickerton, G., Rowland, S.J., Headley, J.V., Scarlett, A.G., West, C.E., Peru, K.M., Parrott, J.L., Conly, F.M. & Hewitt, L.M. (2014). Profiling oil sands mixtures from industrial developments and natural groundwaters for source identification. Environmental science & technology, 48(5), 2660-2670.

Galarneau, E., Hollebone, B. P., Yang, Z. & Schuster, J. (2014). Preliminary measurement-based estimates of PAH emissions from oil sands tailings ponds. Atmospheric environment, 97, 332-335.

Garcia-Aragon, J., Droppo, I. G., Krishnappan, B., Trapp, B. & Jaskot, C. (2011). Experimental assessment of Athabasca River cohesive sediment deposition dynamics. Water Quality Research Journal of Canada, 46(1), 87-96.

Gosselin, P., Hrudey, S. E., Naeth, M. A., Plourde, A., Therrien, R., Van Der Kraak, G. & Xu, Z. (2010). Environmental and health impacts of Canada's oil sands industry. Royal Society of Canada, Ottawa, ON, 10.

Hamrick JM. (2007). The environmental fluid dynamics code theory and computation. Volume 2: sediment and contaminant transport and fate. Tetra Tech, Inc., Fairfax, VA.

Headley, J. V., Akre, C., Conly, F. M., Peru, K. & Dickson, L. C. (2001). Preliminary characterization and source assessment of PAHs in tributary sediments of the Athabasca River, Canada. Environmental Forensics, 2(4), 335-345.

Johnson, D.H., 2008. The application of a two-dimensional sediment transport model in a Cumberland Plateau mountainous stream reach with complex morphology and coarse substrate.

Kashyap, S., Dibike, Y., Shakibaeinia, A., Prowse, T. & Droppo, I. (2017). Two-dimensional numerical modelling of sediment and chemical constituent transport within the lower reaches of the Athabasca River. Environmental Science and Pollution Research, 24(3), 2286-2303.

Khanna, V. (2003). Application of the edg1-d model in the lower Athabasca river basin to estimate high flows during open-water season, contract# 2002–0028. Cumulative Environmental Management Association, Fort McMurray, Alberta.

Kasperski, K.L. (1992). A review of properties and treatment of oil sands tailings. AOSTRA Journal of Research. Alberta Oil Sands Technology Authority. Canada, 8(1).

Kavanagh, R.J., Burnison, B.K., Frank, R.A., Solomon, K.R. & Van Der Kraak, G. (2009). Detecting oil sands process-affected waters in the Alberta oil sands region using synchronous fluorescence spectroscopy. Chemosphere, 76(1), pp.120-126.

Kossoff, D., Dubbin, W., Alfredsson, M., Edwards, S., Macklin, M. & Hudson-Edwards, K. A. (2014). Mine tailings dams: Characteristics, failure, environmental impacts, and remediation. Applied Geochemistry, 51, 229-245.

Kuipers, J. and Vreughdenhil, C. B. 1973. Calculations of two-dimensional horizontal flow. Rep. S 163, Part 1. Delft Hydraulics Laboratory, Delft, The Netherlands.

Langendoen, E.J. and Alonso, C.V., 2008. Modeling the evolution of incised streams: I. Model formulation and validation of flow and streambed evolution components. Journal of Hydraulic Engineering, 134(6), pp.749-762.

Li, C., Fu, L., Stafford, J., Belosevic, M. & El-Din, M. G. (2017). The toxicity of oil sands process-affected water (OSPW): A critical review. Science of the Total Environment, 601, 1785-1802.

Li, C., Singh, A., Klamerth, N.,McPhedran, K., Chelme-Ayala, P., Belosevic, M. & Gamal El-Din, M. (2014). Synthesis of Toxicological Behavior of Oil Sands Process-Affected Water Constituents.

Macklin, M. G., Brewer, P. A., Balteanu, D., Coulthard, T. J., Driga, B., Howard, A. J. & Zaharia, S. (2003). The long term fate and environmental significance of contaminant metals released by the January and March 2000 mining tailings dam failures in Maramureş County, upper Tisa Basin, Romania. Applied Geochemistry, 18(2), 241-257.

MacKinnon, M.D. and Boerger, H., 1986. Description of two treatment methods for detoxifying oil sands tailings pond water. Water Quality Research Journal, 21(4), pp.496-512.

Macklin, M. G., Brewer, P. A., Hudson-Edwards, K. A., Bird, G., Coulthard, T. J., Dennis, I. A., and Turner, J. N. (2006). A geomorphological approach to the management of rivers contaminated by metal mining. Geomorphology, 79(3-4), 423-447.

Mahaffey, A. and Dubé, M., 2017. Review of the composition and toxicity of oil sands process-affected water. Environmental Reviews, 25(1), pp.97-114.

Mahdi, A., Shakibaeinia, A., & Dibike, Y. B. (2020). Numerical modelling of oil-sands tailings dam breach runout and overland flow. Science of the Total Environment, 703, 134568.

Martin, J.L., McCutcheon, S.C. and Schottman, R.W., 2018. Hydrodynamics and transport for water quality modeling. CRC press.

Mashriqui, H.S., 2003. Hydrodynamic and sediment transport modeling of deltaic sediment processes. Louisiana State University and Agricultural & Mechanical College.

McQueen, A.D., Kinley, C.M., Hendrikse, M., Gaspari, D.P., Calomeni, A.J., Iwinski, K.J., Castle, J.W., Haakensen, M.C., Peru, K.M., Headley, J.V. and Rodgers Jr, J.H., 2017. A risk-based approach for identifying constituents of concern in oil sands process-affected water from the Athabasca Oil Sands region. Chemosphere, 173, 340-350.

O'Brien, J., & Julien, P. (2000). Flo-2D user's manual, version 2000.01. Nutrioso, AZ, USA: Flo Engineering.

Olías, M., Moral, F., Galván, L., & Cerón, J. C. (2012). Groundwater contamination evolution in the Guadiamar and Agrio aquifers after the Aznalcóllar spill: assessment and environmental implications. Environmental monitoring and assessment, 184(6), 3629-3641.

Papanicolaou, N. A., Elhakeem, M., Krallis, G. and Prakash, S., 2008. Sediment transport modeling review—current and future developments. American Society of Civil Engineers.

Petticrew, E.L., Albers, S.J., Baldwin, S.A., Carmack, E.C., Déry, S.J., Gantner, N., Graves, K.E., Laval, B., Morrison, J., Owens, P.N. and Selbie, D.T., 2015. The impact of a catastrophic mine tailings impoundment spill into one of North America's largest fjord lakes: Quesnel Lake, British Columbia, Canada. Geophysical Research Letters, 42(9), pp.3347-3355.

Pietroniro, A., Hicks, F., Andrishak, A., Watson, D., Boudreau, P., & Kouwen, N. (2011). Hydraulic routing of flows for the Mackenzie River. Environment Canada, University of Alberta & National Research Council of Canada.

Prudhomme, C. and Davies, H. 2009. Assessing uncertainties in climate change impact analysses on the river flow regimes in the UK. Part 1: baseline climate change. 93: 177-195.

Riahi, K., Rao, S., Krey, V., Cho, C., Chirkov, V., Fischer, G., Kindermann, G., Nakicenovic, N. and Rafaj, P. (2011). RCP 8.5—A scenario of comparatively high greenhouse gas emissions. Climatic change. 109(1): pp.33-57.

Rudolph, T., & Coldewey, W. G. (1971). Implications of earthquakes on the stability of tailings dams. In.

Shakibaeinia, A., Dibike, Y. B., Kashyap, S., Prowse, T. D., & Droppo, I. G. (2017). A numerical framework for modelling sediment and chemical constituents transport in the Lower Athabasca River. Journal of Soils and Sediments, 17(4), 1140-1159.

Shakibaeinia, A., Kashyap, S., Dibike, Y. B., & Prowse, T. D. (2016). An integrated numerical framework for water quality modelling in cold-region rivers: A case of the lower Athabasca River. Science of the Total Environment, 569, 634-646.

Smolders, A., Lock, R., Van der Velde, G., Medina Hoyos, R., & Roelofs, J. (2003). Effects of mining activities on heavy metal concentrations in water, sediment, and macroinvertebrates in different reaches of the Pilcomayo River, South America. Archives of Environmental Contamination and Toxicology, 44(3), 0314-0323.

Siwik, P.L., Van Meer, T., MacKinnon, M.D. and Paszkowski, C.A., 2000. Growth of fathead minnows in oilsand-processed wastewater in laboratory and field. Environmental Toxicology and Chemistry: An International Journal, 19(7), pp.1837-1845.

Stasik, S., Loick, N., Knöller, K., Weisener, C. and Wendt-Potthoff, K., 2014. Understanding biogeochemical gradients of sulfur, iron and carbon in an oil sands tailings pond. Chemical Geology, 382, pp.44-53.

Syncrude Canada Ltd, 2010. Baseline Survey for Fluid Deposits: Syncrude Mildred Lake and Aurora North Retrieved from Alberta Energy Regulator Website: http://www.aer.ca/rules-and regulations/directives/tailings-plans- 2012.

Taylor, K. E., Stouffer, R. J., & Meehl, G. A. (2012). An overview of CMIP5 and the experiment design. Bulletin of the American meteorological Society, 93(4), 485-498.

Tetra Tech, 2007. The Environmental Fluid Dynamics Code Theory and Computation. Volume 1: Hydrodynamics and Mass Transport.

Thomas, W.A. and Prasuhn, A.L., 1977. Mathematical modeling of scour and deposition. Journal of the Hydraulics Division, 103(8), pp.851-863.

Thomas, W. A. and McAnally, W. H. 1990. "Open channel flow and sedimentation, TABS-MD," IR-HL-85-1, revised, U.S. Army Engineer Waterways Experiment Station, Vicksburg, MS.

Timoney, K.P. and Lee, P. 2009. Does the Alberta tar sands industry pollute? The scientific evidence. The Open Conservation Biology Journal, 3(1): 65-81.

Trenberth, KE., Jones, PD., Ambenje, P., Bojariu, R., Easterling, D., Klein Tank, A., Parker, D., Rahimzadeh, F., Renwick, JA., Rusticucci, M., Soden, B., & Zhai, P. (2007). Observations: Surface and atmospheric climate change. In S. Solomon, D. Qin, M. Manning, Z. Chen, M. Marquis, KB. Averyt, M. Tignor, & HL. Miller (Eds.), Climate Change 2007: The Physical Science Basis. Contribution of Working Group 1 to the 4th Assessment Report of the Intergovernmental Panel on Climate Change Cambridge University Press.

Teng, J., Chiew, S. and Vaze, J. 2012. Estimation of climate change impact on mean annual runoff across continental Australia using Budykoand Fu equations and hydrological models. Journal of Hydrometeorol. 43: 1094–1106. doi:10.1175/JHM-D-11-097.

Turner, J., Brewer, P., & Macklin, M. (2008). Fluvial-controlled metal and As mobilisation, dispersal and storage in the Río Guadiamar, SW Spain and its implications for long-term contaminant fluxes to the Doñana wetlands. Science of the Total Environment, 394(1), 144-161.

Turner, J. N. (2003). A Geomorphological-Geochemical Assessment of the Impacts of the Aznalcollar Tailings Dam Failure on the Rio Guadiamar, Southwest Spain. University of Wales.

Van den Heuvel, M.R., Hogan, N.S., Roloson, S.D. and Van Der Kraak, G.J., 2012. Reproductive development of yellow perch (Perca flavescens) exposed to oil sands–affected waters. Environmental Toxicology and Chemistry, 31(3), pp.654-662.

van Heerden, L. I., 1980. Sedimentary responses during flood and non-flood conditions, new Atchafalaya delta, Louisiana. MS Thesis, Dept. Marin Science, Louisiana State University, Baton Rouge, LA.

Van Rijn, L.C., 1984. Sediment transport, part II: suspended load transport. Journal of hydraulic engineering, 110(11), pp.1613-1641.

Van Vuuren, D.P., Edmonds, J., Kainuma, M., Riahi, K., Thomson, A., Hibbard, K., Hurtt, G.C., Kram, T., Krey, V., Lamarque, J.F. and Masui, T. (2011a.) The representative concentration pathways: an overview. Climatic change. 109(1): pp.5-31.

Van Vuuren, D.P., Edmonds, J.A., Kainuma, M., Riahi, K. and Weyant, J. (2011b). A special issue on the RCPs. Climatic Change. 109(1): pp.1-4.

Voldoire, A., Sanchez-Gomez, E., Salas y Mélia, D., Decharme, B., Cassou, C., Sénési, S., . . . Chevallier, M. (2013). The CNRM-CM5. 1 global climate model: description and basic evaluation. Climate dynamics, 40(9), 2091-2121.

Wang, B. Liu, D.L. Asseng, S. Macadam, I and Yu, Q. (2015): Impact of Climate Change on Wheat floe Ring time in Saetern Australia. Agriculture and Forest Meteorology 209-210:11- 21.

Wiklund, J.A., Hall, R.I., Wolfe, B.B., Edwards, T.W., Farwell, A.J. and Dixon, D.G., 2014. Use of pre-industrial floodplain lake sediments to establish baseline river metal concentrations downstream of Alberta oil sands: a new approach for detecting pollution of rivers. Environmental Research Letters, 9(12), p.124019.

WISE World Information Service on Energy Uranium Project, 2012. Chronology of Major Tailings Dam Failures. <http://www.antenna.nl/wise/uranium/ mdaf.html> (accessed 12.11.12).

Welder, F. A. 1959. Processes of deltaic sedimentation in the lower Mississippi River. Tech. Report No. 12. Coastal Studies Institute, Louisiana State University, Baton Rouge. LA. 90 pp.

Wong, M. and Parker, G. 2006. Reanalysis and Correction of Bed-Load Relation of Meyer-Peter and Müller Using Their Own Database. Journal of Hydraulic Engineering. 132 (11): 1159-1190. DOI: 10.1061/(ASCE)0733-9429(2006)132:11(1159).

World Bank. 2021. Tailings Storage Facilities. Good Practice Note on Dam Safety; Technical Note 7. World Bank, Washington, DC. https://openknowledge.worldbank.org/handle/10986/35491 License: CC BY 3.0 IGO.

Wrona, F. J., Carey, J., Brownlee, B., & McCauley, E. (2000). Contaminant sources, distribution, and fate in the Athabasca, Peace and Slave River Basins, Canada. Journal of Aquatic Ecosystem Stress and Recovery, 8(1), 39-51.

Wu, Weiming. (2008). Computational River Dynamics. Taylor & Francis – Balkema, Leiden, The Netherlands.

Wu, W., Vieira, D.A. and Wang, S.S., 2000. New capabilities of the CCHE1D channel network model. In Building Partnerships (pp. 1-10).

Younger, P. L., & Wolkersdorfer, C. (2004). Mining impacts on the fresh water environment: technical and managerial guidelines for catchment scale management. Mine water and the environment, 23, s2.

Zorkeflee, A.H., Aminuddin, A. G. and Nor, A. Z. 2004. Application of 2-D Modelling for Muda River Using CCHE2D. 2nd International Conference on Managing Rivers in the 21st Century: Solutions Towards Sustainable River Basins. 249-253.

Appendix A Investigating climate change scenarios

According to the three climate model scenarios (CanESM SD45, CanESM SD85, and CNRM SD45), the simulation was repeated based on each future scenario to provide a range of uncertainty in the result. Figure 1 and 2 shows simulated time series of depth-averaged water column sediment concentration and Lead concentration for the three climate model scenarios (CanESM SD45, CanESM SD85, and CNRM SD45) in scenario 6 (SN6: Spill happens in an average future flow condition). In all scenarios, the maximum sediment concentration in the water column occurs at approximately the same time, and almost all three climate model scenarios show a general trend. In all climate model scenarios, peak sediment concentrations downstream of the P1 and P2 junctions (DS spill location) occur on day 0.3, and downstream of the confluence of the Firebug River to the LAR (DS Firebag) happens on day 1.1.

In Figures 1 and 2, Scenario 6 shows that the speedy increase in the concentration of sediment and lead in the proximity of the spill site starts from the T=0 day and reaches the release concentrations of about 380 g /l and 3 mg /l, respectively. Then, 48 hours later, they reach downstream of the study area and after about 70 hours from the start, it comes out completely from downstream. It can also be seen from the release points downstream that the concentration of the water column gradually decreases, this is because part of the sediments and chemicals settle in the riverbed. Still, the peak occurs on day 0.2 or 0.3 because the effect of the backwater effect together with advection/dispersion mechanisms causes these concentrations to be transported upstream for several kilometers and re-flow downstream (Dibike et al., 2018). In the following study, Due to the slight difference between the results of climate model scenarios the Canadian model with the high emission scenario of CanESM SD85 was used for data analysis.

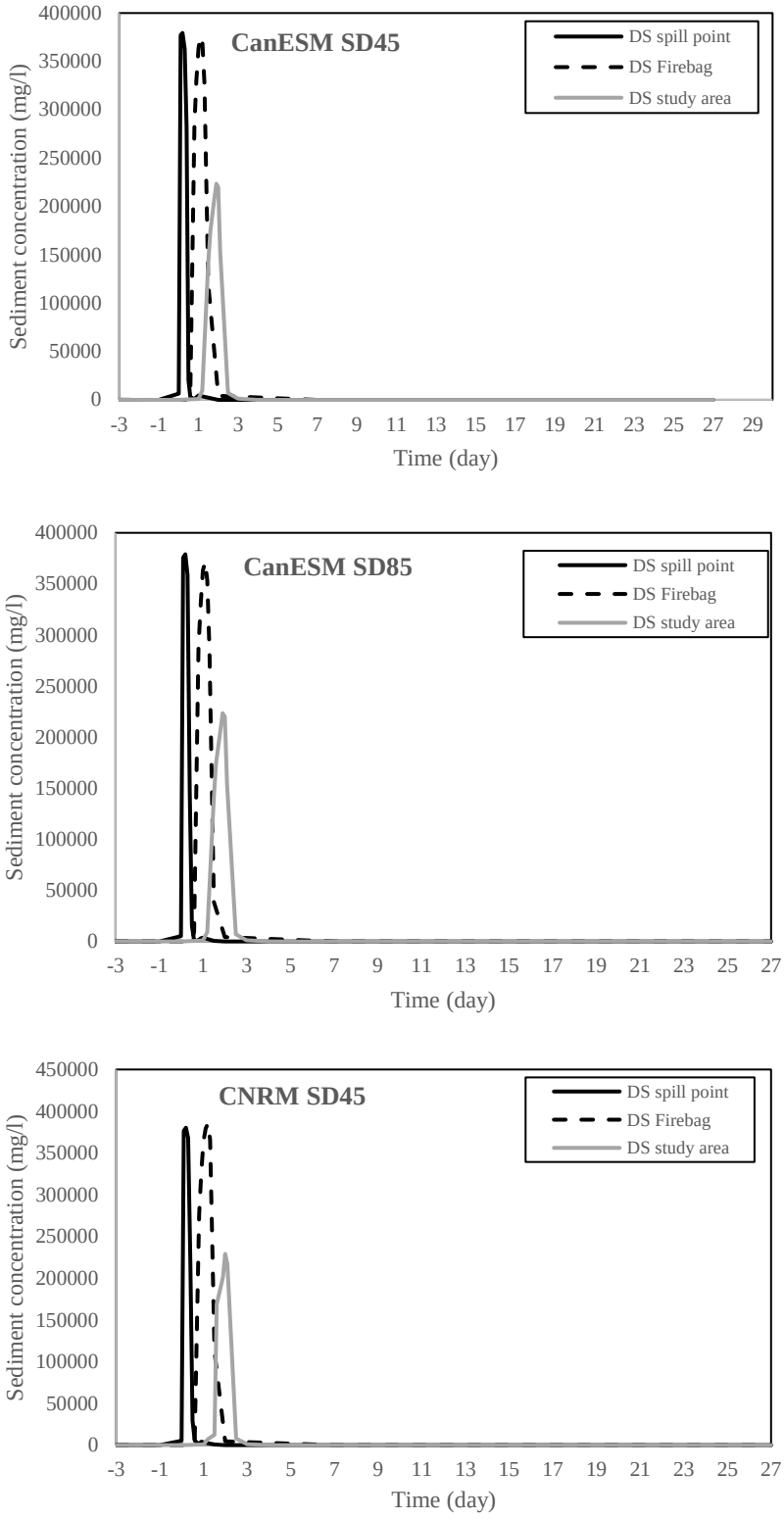

Figure 4 simulated time series of sediment concentration in the depth-averaged water column under scenario 6 regarding the three climate model scenarios

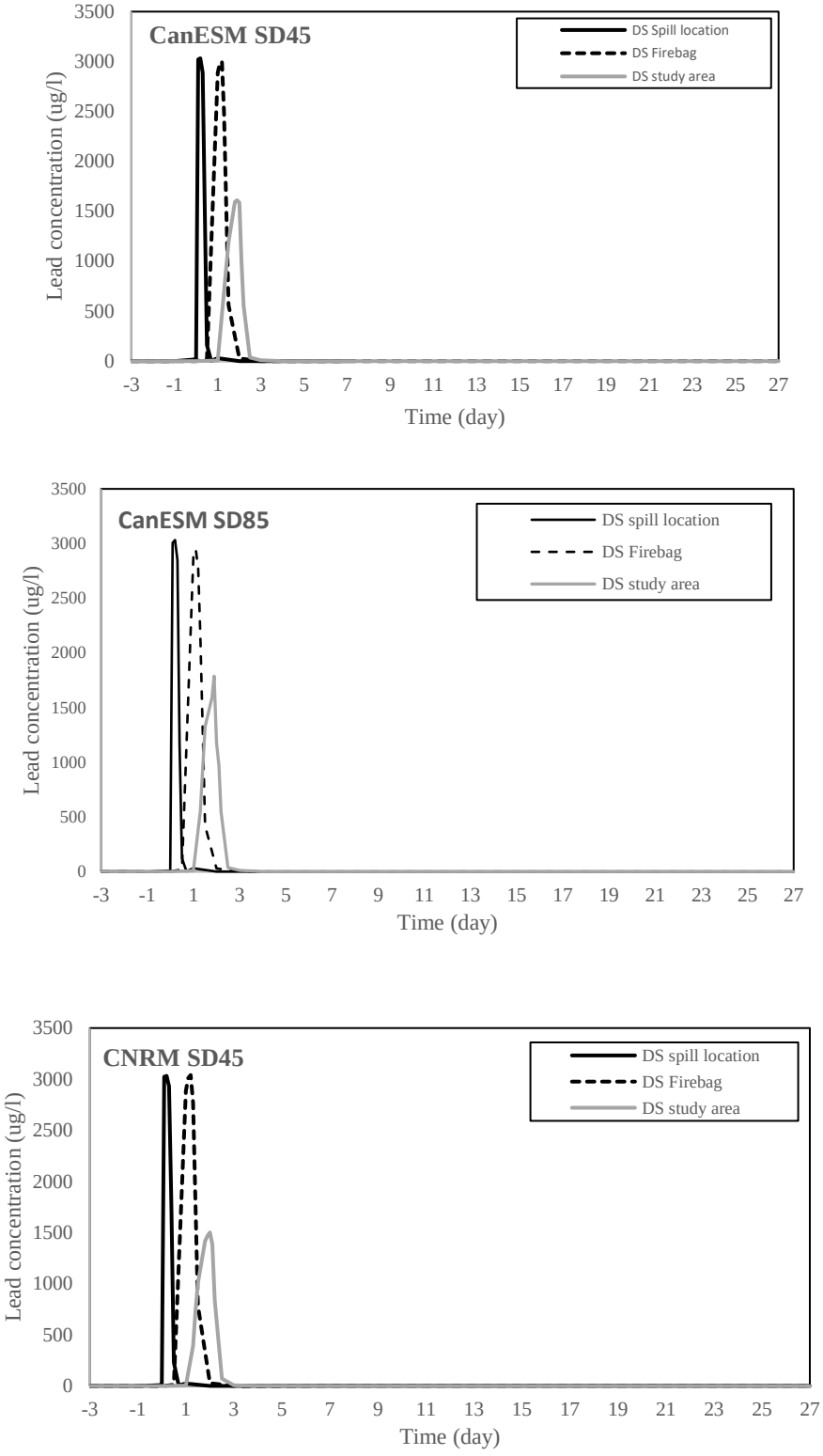

Figure 2 simulated time series of Lead concentration in the depth-averaged water column under scenario 6 regarding the three climate model scenarios

These sediments/toxins deposited in the riverbed downstream may return to the water column by flooding from upstream and are transferred for miles. Therefore, in scenarios 9 and 10, a flood wave with a return period of 25 years and 50 years, respectively, was considered in future data after 15 days of the spill, and the results are shown in Figures 3 and 4. After the peak flow in the return periods of 25 years and 50 years, concentration was constant more or less, but with the occurrence of floods on the 12th day from the beginning of the tailings spill, the flow rate increased and the concentration in the water column along the LAR increased. In both scenarios, from day 12.3, an increase in the concentration of the water column is observed, which is transferred to the downstream and after 48 hours is completely out of the study area downstream. The highest concentration of suspended solids in the water column occurs to 250 mg / l per day at 80 km upstream (Figure 4).

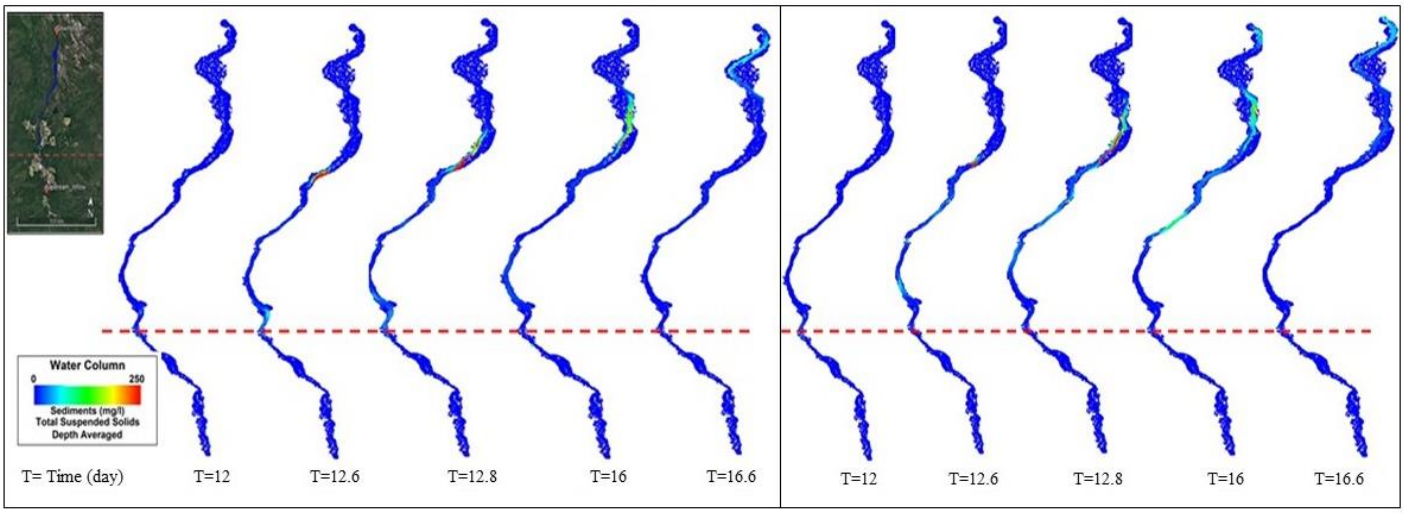

Figure 3 the time sequence of simulated Total Suspended Solids (TSS) in the depth-averaged water column after a flood on the 15th day based on scenario 9 (left) and scenario 10 (right)

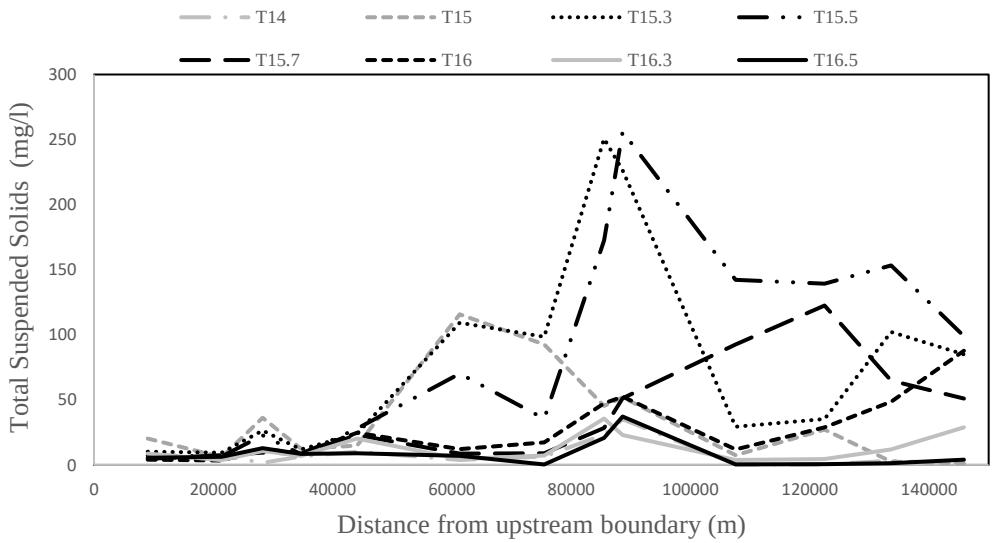

Figure 4 the amount of Total Suspended Solids (TSS) for scenario 9 at some distances from the upstream boundary (T is time and by day)